Graph Theoretical analysis and *in silico* modeling and molecular dynamic studies of fused indolin-2-one derivatives for the treatment of inflammation

Panneerselvam Theivendren (✉ tpsphc@gmail.com)
  Swamy Vivekananda College of Pharmacy   https://orcid.org/0000-0002-8197-4688

Selvaraj Kunjiappan
  Kalasalingam University: Kalasalingam Academy of Research and Education

Parasuraman Pavadai
  MS Ramaiah College of Pharmacy: MS Ramaiah University of Applied Sciences

Saravanan Govindaraj
  MNR College of Pharmacy

Murugananthan Gopal
  Swamy Vivekananda College of Pharmacy

Sudhakar Pachiappan
  Swamy Vivekananda College of Pharmacy

Yashoda Mariappa Hegde
  Swamy Vivekananda College of Pharmacy

Nivetha Shanmugam
  Swamy Vivekananda College of Pharmacy

Abstract

In the present work, novel 3-(4-(5-(substituted phenyl)-3-phenyl-4,5-dihydro-1H-pyrazole-1-carbonyl)phenylimino)-1-(substitutedmethyl)indolin-2-one derivatives were obtained *via* the reaction of 4-(1-(substituted methyl)-2-oxoindolin-3-ylideneamino) benzohydrazide with appropriate aromatic chalcone. The synthesized compounds were investigated for their *in silico* chemokine/CXCR6 inhibitory activity. The most effective chemokine inhibitors were also evaluated for their *in vivo* antiinflammatory activity. The 3-(4-(5-(4-Chlorophenyl)-3-phenyl-4,5-dihydro-1*H*-pyrazole-1-carbonyl) phenylimino)-1-(morpholino methyl) indolin-2-one (**5a**) derivative showed significant chemokine inhibition with eleven amino acid interaction as compared with standard Acetaminophen whereas Celecoxib, Diclofenac, Indomethacin, Naproxen, Ibuprofen, Aspirin showed less amino acid interaction. Based on the theoretical study reports the *in vivo* antiinflammatory activity was performed for the 3-(4-(5-(substituted phenyl)-3-phenyl-4,5-dihydro-1H-pyrazole-1-carbonyl)phenylimino)-1-(substitutedmethyl)indolin-2-one (**5a-5l**). The observed results of *in vivo* study indicate that the compounds **5a**, **5c** exhibited significant antiinflammatory activity.

Introduction

Chemokines are a group of cytokines that regulate staffing of leukocyte and a term derived from "chemotactic cytokines," were given to these tiny (8–14 kDa) proteins. These chemokines share conserved sequences and four conserved cysteines joined by disulfide bonds. The arrangement of cysteine residues at the NH_2 terminus of chemokines is separated into four groups that are CC, CXC, C, and CX3C, where X signifies a separating amino acid. Inflammatory chemokines, that are raised in inflammatory circumstances. Chemokines are created in response to inflammatory cytokines, and they preferentially attract monocytes, lymphocytes, and neutrophils by activating G-protein-coupled receptors, resulting in chemotaxis [1]. Chemokines that bind to promiscuous cCKRs and ACKRs (i.e., CCR1, CCR2, CCR3, CCR5, CXCR1, CXCR2, CXCR3, ACKR1, and ACKR2) are frequently seen in these inflammatory chemokine patterns[2]. Many inflammatory diseases in humans have been linked to complicated chemokine expression patterns. CXCR6 neutralisation protects against a variety of inflammatory challenges, including lung ischemia-reperfusion injury, pleuritis, and glomerulonephritis, which is consistent with CXCR6's close association with neutrophil-mediated inflammatory diseases like bacterial pneumonia and ischemia-reperfusion injury. Chemokines have sparked a lot of interest as potential therapeutic targets because of their critical function in inflammation[3]. Chemokine inhibition is a viable strategy for pharmacological intervention in inflammation. Nonsteroidal anti-inflammatory medications (NSAIDs) are a class of medicinal agents that work by blocking the production of chemokines Fig. 1. Long-term use of nonsteroidal anti-inflammatory medicines (NSAIDs) can cause serious gastrointestinal adverse effects, limiting their use. The harmful effects of nonselective NSAIDs are caused by the suppression of chemokines, which results in a decrease in the amounts of beneficial prostaglandins in the gastrointestinal (GI) tract. Heterocycle-fused scaffolds, being one of the most favoured structures in drug discovery, demonstrate a wide range of biological activities, allowing them to operate as anti-inflammatory, anti-cancer, antipsychotic, and anti-diabetic drugs[4–9]. Indoline is a common type of heterocycle-fused scaffold that has a wide range of pharmacological applications, including anti-inflammatory properties. Based on the foregoing, the current study aimed to investigate the relationships between chemical structure and antiinflammatory activity of 3-(4-(5-(substituted phenyl)-3-phenyl-4,5-dihydro-1H-pyrazole-1-carbonyl) phenylimino)-1-(substituted methyl) indolin-2-one (5a-5l) heterocyclic derivatives, as well as their mechanism of action.

Materials And Methods

Materials

The chemicals and reagents used were obtained from various chemical units Qualigens, E. Merck India Ltd., CDH, and SD Fine Chem. These solvents used were of LR grade and purified before their use. The silica gel G used for analytical chromatography (TLC) was obtained from E. Merck India Ltd. All the melting points were taken in open glass capillary and are uncorrected. ^{1}H-NMR spectra were recorded at 500 MHz on Bruker Avance-500 NMR spectrometer in $CDCl_3$ using tetramethylsilane (TMS) as an internal standard. The chemical shifts are reported in ppm scale. Mass spectra were obtained on a JEOL-SX-102 instrument using electron impact ionization. All the IR spectra were recorded in KBr pellets on a Jasco FT-IR 410 spectrometer. Elemental analyses were performed on a Perkine Elmer model 2400C analyzer and were within ± 0.4 % of the theoretical values.

Methods

Graph Theoretical Analysis

The network of protein interaction (hsa: 04062) in homo sapiens was chosen to recognize the influential proteins, and the Kyoto Encyclopedia of Genes and Genomes database https://www.genome.jp/pathway/hsa04062 was used for graph theoretical analysis[9, 10].

Druglikeness Analysis

For all of the test compounds **5a-5l**, druglikeness analysis was performed, which is a complex balancing of multiple chemical features and structure factors that determines whether a molecule is related to previously recognized drugs. The Molinspiration online tool was utilized to perform druglikeness analysis [11] https://www.molinspiration.com/docu/miscreen/druglikeness.html

Protein Preparation

The Protein Data Bank of the Research Collaboratory for Structural Bioinformatics (RCSB) (PDB: 6KVA) https://www.rcsb.org/ was used to obtain the X-ray crystal structures of the chemokine receptor complex with CXCR6 for this study. The protein was pre-processed using the CHARMM-GUI programme (https://www.charmm-gui.org/) to add missing residue and remove superfluous ligand and water molecules [12].

Ligand Preparation

The synthetic 3-(4-(5-(substituted phenyl)-3-phenyl-4,5-dihydro-1H-pyrazole-1-carbonyl) phenylimino)-1-(substitutedmethyl)indolin-2-one (5a-5l) test substance, as well as the standards Acetaminophen, Celecoxib, Diclofenac, Indomethacin, Naproxen, Ibuprofen against CXCR6, sdp files were collected by using public database PubChem (https://pubchem.ncbi.nlm.nih.gov/).

The collected test compound and standards were pre-processed for the preparation of cluster by using *BIOVIA Discovery Studio Visualizer* tool https://discover.3ds.com/discovery-studio-visualizer-download.

Docking Protocol

To complete intermediate steps such as protein and ligand preparation pdbqt files, the AutoDock vina-PyRx programme was used, and the configuration file contained protein and ligand information as well as grid box settings. The AutoDock vina-PyRx tool was used to give the protein polar hydrogen, solvation parameters, and fragmental volumes. The grid map, which contained a grid box, was created using AutoGrid. The grid centre was given dimensions (x,y,z). To reduce time on computation, the ligand structure is used to create a score grid. In AutoDock vina-PyRx/Vina, which

uses iterated local search global optimise, both the protein and the ligands are considered stiff throughout the docking stage. The data were merged and represented by the findings with the lowest free energy of binding, with the exception of 1.0A in positional root-mean square deviation. The posture with the lowest binding energy or affinity was identified for future research, and the amino acid interaction was visualised using the BIOVIA Discovery Studio Visualizer tool.

Binding site identification

In order to carry out a chemical process, an enzyme or protein must have a binding site where it may bond to a target molecule. The key strategy that we have to ensure adequate and favourable catalytic regions supports bioactive compounds in creating sufficient contact sites for strong engagement with target enzymes is the binding of ligands or bioactive substances to a protein or enzyme's specific location. We were able to find all of the target compounds' active binding sites using the Prank Web server (https://prankweb.cz/). The AutoDock vina-PyRx tool was used to generate a receptor grid after finding the protein's active site.

In vivo antiinflammatory activity

The antiinflammatory effect was assessed using the carrageenan-induced mouse paw edema paradigm, which was previously described method [13]. In a batch of 10 mice (body weight 19-21 g each), inflammation was generated by injecting a 1 percent solution of carrageenan lambda (sigma) dissolved in a 0.5 percent saline solution containing 2.5 percent Tween 80 into the right hind paw. After 30 minutes, the compounds were given intraperitoneally to a group of mice at a dose of 250 mg kg^{-1}. The standard antiinflammatory medicine was ASA, which was given at a dose of 250 mg kg^{-1}. Despite the discovery of numerous new medicines, standard Diclofenac Celecoxib remains the most often given analgesic, antipyretic and antiinflammatory agent in medicine, and it is used to evaluate new pharmaceuticals in pharmacological assays. The title work Graph Theoretical analysis and in silico modeling and molecular dynamic studies of fused indolin-2-one derivatives for the treatment of inflammation work was reviewed by IAEC members and approved SVCP/IAEC/PA/02/02/2022.

Density functionality theory

The PubChem public database (https://pubchem.ncbi.nlm.nih.gov/) was used to obtain the synthesized test compound 5a, 5c, and standard Celecoxib sdp files, which were then placed into the Spartan14 Graphical User Interface tool for energy minimization. It was also introduced to GaussView 6.0.16 so that Hatree energy estimations for HOMO and LUMO may be obtained. The measured Hatree energy values must be converted into electron volt energy values in order to calculate the HOMO and LUMO energy gaps. The stability of the test compound, standard, and reference compound is represented by the energy gap [14].

Simulation-based drug metabolism and pharmacokinetic modelling

In silico ADME and physicochemical property predictions were utilised to analyse the overall potency and efficacy of the 5a, 5c, and standard Celecoxib. The SwissADME online server (http://www.swissadme.ch/) was used to examine molecular weight, molar refractivity, solubility, bioavailability and bioavailability radar map, egg boiled model, brain penetration, and human gastro intestinal absorption. The SwissADME is a free website that assists researchers in predicting the pharmacokinetic and drug-likeness properties of test standards and references [11].

Synthesis

A mixture of isatin (1.47 g; 0.01 mol), formaldehyde (0.45 g; 0.015 mol), and morpholine/piperidine (0.87/0.85 g; 0.01 mol) in ethanol (25 ml) was stirred for 2 h in magnetic stirrer. Then the resulting mixture was refluxed on water bath for

4 h. The above mixture was poured on crushed ice and mixed well. The solid **2a/2b** which obtained was filtered, dried, and recrystallised using rectified spirit. Equimolar quantity of 1-(substitutedmethyl)indoline-2,3-dione **2a/2b** (2.46/2.44 g; 0.01 mol)and *p*-amino benzoic acid (1.37 g; 0.01 mol) in ethanol (30 ml) was refluxed on sand bath for 5 h. The reaction mixture was cooled to room temperature, poured in crushed ice and kept aside overnight in refrigerator. The product separated **3a/3b** was filtered, dried and recrystallised using ethanol. To 4-(1-(substitutedmethyl)-2-oxoindolin-3-ylideneamino)benzoicacid **3a/3b** (3.65/3.63 g; 0.01 mol), thionyl chloride (1.78 g; 0.015 mol) was added slowly with stirring and refluxed gently for 2 h. The excess of thionyl chloride was distilled off, and the reaction mixture was cooled in ice bath. The product thus formed was immediately used for next step. To the above product, ethanol (50 ml) was added. To this solution 95 % hydrazine hydrate (1 g; 0.02 mol) was slowly added with stirring. Then the mixture was refluxed for 10 h followed by removal of excess solvent under reduced pressure, and resultant solution was poured in ice cold water. The product separated **4a/4b** was filtered, and recrystallised from ethanol. Equimolar quantity of various aromatic/heterocyclic aldehydes (0.01 mol) and acetophenone (1.20 g; 0.01 mol) was dissolved in minimum quantity of ethanol. To this mixture, a catalytic quantity of sodium hydroxide pellet was added. Then the reaction mixture was stirred for 2-8 h and poured on ice cold water. The product separated (chalcone) was filtered, dried and utilized for further step. Various aromatic chalcone (0.01 mol) was added to the 4-(1-(substitutedmethyl)-2-oxoindolin-3-ylideneamino)benzohydrazide **4a/4b** (3.79/3.77 g; 0.01 mol) in round bottom flask containing *N,N*-dimethyl formamide (50 ml). The above mixture was refluxed in oil bath for a period of 12 h. Then the reaction mixture was cooled, poured in to a beaker containing ice cold water, and kept aside for 24 h. The obtained product **5a-5l** was separated by filtration, dried over the filter paper, and recrystallised using ethanol.

Results And Discussion

Graph theoretical analysis

Proteins (nodes) and interactions (edges) were re-created as a graph, which was depicted in **Figure 2** and **Table 1**. The network has 59 nodes and 82 edges, and the characteristics were used to determine the relevance of proteins. CXCR6/Chemokine, FGR, PIK3CA, PTK2, GNB5, CDC42, AKT3, HRAS, RAC1, PIK3R6, PLCB1, GNAI1, VAV3, ITK, PRKCB, PRKCZ, RASGRP2, PTK2B, and PREX1 are high significant proteins based on the average measure of each parameter. CXCR6/Chemokine had a Centrality score of 2262 for Stress, a score of 9 for Radiality, a score of 0.439326 for Eigenvector, a score of 0.125 for Eccentricity, a score of 0.007299 for Closeness, a score of 944.0443 for Betweenness, and a score of 12 for Degree from the network among the best 19 nodes. Based on significant metrics with its threshold values, the target CXCR6/Chemokine was identified as a therapeutic target for the treatment of inflammation. Because of its interaction with 19 main proteins that are involved in inflammation, CXCR6/Chemokine has gotten increasing attention. CXCR6/Chemokine was picked as a noteworthy target based on the graph theoretical analysis report and importance.

Druglikeness analysis

The activity scores for the drug relative to "average drug-like molecules" are displayed in the **Figure 3**. The greater the value of the score, the more likely it is that the particular molecule will be active. The analysis report was conforming that the chosen **5a-5l** test compounds were having kinase protein inhibitory activity.

Insilico Modelling

Molecular docking studies of was carried out with the synthesized 3-(4-(5-(substituted phenyl)-3-phenyl-4,5-dihydro-1H-pyrazole-1-carbonyl) phenyl imino)-1-(substitutedmethyl)indolin-2-one (**5a-5l**) test substance, as well as the standards Acetaminophen, Celecoxib, Diclofenac, Indomethacin, Naproxen, Ibuprofen against CXCR6 (PDB: 6KVA). Among tested

ligands **5a, 5c,** and standardCelecoxib showed high amino acid interaction and significant binding affinity towards CXCR6 protein with the biding energy of -11.4, -11.0 and -8.8 Kcal/mol respectively. The amino acids interaction with the **5a** was ARG39[2.64 Å], ARG86[3.06 Å, 4.71Å], LEU87[3.14 Å], ARG88[3.96 Å], ASP90[4.05 Å], GLNP111[3.13 Å,11.72Å], VAL154[2.63 Å],THR155[3.68 Å],VAL156[2.10 Å]. The amino acids interaction with the **5b** was GLN1[3.12 Å], PRO46[3.15 Å], PHE106 [16.51 Å,3.15Å], GLY108[3.52 Å], GLN179[4.12 Å], SER180[3.78 Å], SER185[3.19 Å]. The amino acids interaction with the **5c** was GLN1[2.00 Å, 3.31 Å, 3.31 Å, 4.53 Å, 15.37 Å], PRO42[3.94 Å], GLU47[3.55 Å], LYS64[3.59 Å], TRP104[3.32 Å], VAL105[3.14 Å],PHE106[2.16 Å]. The amino acids interaction with the **5d** was GLN6[3.59 Å], ARG39[5.17 Å], ALA41[2.87 Å], GLY45[, 2.24 Å 2.97 Å], GLU47[3.19 Å , 3.84 Å], GLY108[3.33 Å]. The amino acids interaction with the **5e** was GLN44[2.39 Å, 2.39 Å, 3.51 Å], ASP90[4.75 Å], VAL154[3.88 Å], VAL169[3.84 Å], THR171[11.12 Å]. The amino acids interaction with the **5f** was ARG88[5.12 Å], PRO89[5.00 Å], ASP90[4.26 Å], GLY152[2.87 Å], ALA153[3.51 Å], THR171[3.80 Å]. The amino acids interaction with the **5g** was GLN1 [2.05 Å, 3.69 Å], GLU47 [3.72 Å], LYS64 [4.59 Å, 5.06 Å], TRP104[3.64 Å], THR173[3.50 Å], ALA176[3.04 Å]. The amino acids interaction with the 5h was GLN1[3.25 Å], ARG39[2.78 Å], GLN44[2.29 Å], GLY45[2.71 Å], GLU47[3.64 Å], ASP90[3.31 Å], GLP168[3.37 Å], SER180[2.67 Å]. The amino acids interaction with the **5i** was GLP40[2.49 Å, 3.93 Å], GLY43[4.18 Å, 3.71 Å], GLN44[2.45 Å], ASP93[3.65 Å], TYR96[1.88 Å]. The amino acids interaction with the **5j** was TRP158[1.26 Å], VAL165[1.93 Å], LYS166[3.67 Å], TYR184[5.48 Å]. The amino acids interaction with the **5k** was GLN44 [2.36 Å, 3.24 Å], GLU47[3.49 Å], ASP90[4.70 Å], VAL154[3.85 Å, 3.00 Å], VAL169[3.80 Å], THR171[11.18 Å]. The amino acid interaction with the **5l** was GLP40 [2.46 Å, 4.00 Å], GLY43[3.78 Å], GLN44[2.62 Å], ASP93[3.57 Å],VAL94[3.81 Å], TYR96[1.97 Å], LYS166[2.29 Å]. The amino acids interaction with the Celecoxib was GLN1[4.16 Å], LEU4[3.03 Å], GLU47[4.26 Å,4.26 Å], TRP48[2.25 Å], TRP104[1.95 Å], PHE106[3.04 Å, 3.80 Å, 2.99 Å], GLY108[2.89 Å], SER180[2.97 Å]. The amino acids interaction with the Aspirin was ARG34[4.83 Å, 2.97 Å], TRP99[3.06 Å].The amino acids interaction with the Acetaminophen was HSD100[2.21 Å], VAL119[2.88 Å], SER121[1.96 Å]. The amino acids interaction with the Diclofenac was ALA2[3.28 Å], PRO46[4.07 Å], TRP48[2.11 Å], GLN63[2.46 Å], TRP104[3.36 Å, 4.03 Å], VAL105[3.90 Å, 3.99 Å]. The amino acids interaction with the Ibuprofen was GLN1[2.39 Å], ARG25[15.81 Å], SER121[2.16 Å], ALA122[2.14 Å]. The amino acids interaction with the Indomethacin was GLN1[2.67 Å], PRO46[2.96 Å], GLU47[3.40 Å, 4.00 Å], PHE106[3.27 Å], GLY107[2.21 Å]. The amino acids interaction with the Naproxen was ARG25[15.76 Å], HSD100[3.29 Å], SER120[2.70 Å], SER121[2.27 Å], ALA122[2.25 Å]. The binding interactions, 2D and 3D model of 5a, 5c, and Celecoxib were shown in the **Table 2** and Figure **4-6**.

In vivo antiinflammatory activity

Antiinflammatory tests have been performed for compounds **5a-5l** and standard Diclofenac Celecoxib by using groups of Swiss albino mice at the dose of 250 mg kg^{-1}. All of the tested compounds were exhibited antiinflammatory activity compared with the standards. Both of these standards were commercially available and also it was used for relating purposes with dose level of 250 mg kg^{-1}. Compound **5a** showed the highest activity reducing the paw edema by 74.2%. Pyrimidines 5c and 5l presented 48.1% and 40.4% of inflammation reductions, respectively (**Table 3**, **4** and **Figure 7**).

Density functionality theory

The stability and bioactive nature of 5a, 5c, and Celecoxib was measured by using energy values of HOMO and LUMO. From the energy values of HOMO and LUMO, the energy gap was calculated to measure the stability and bioactivity of test compound, and standard. The test compound **5a** HOMO energy value was 0.28634, LUMO energy value was 0.21216 and HOMO and LUMO energy gap was 2.018541652. Likewise the **5c** HOMO and LUMO energy gap was 1.98776355 and Celecoxib HOMO and LUMO energy gap was 3.57253219. Based on the obtained data was suggesting that the test compounds was having significant stability as par with the standard. The energy values of HOMO and LUMO of test compound, and standard were shown in the **Table 5** and **Figure 8-10**

Pharmacokinetic and physicochemical properties prediction analysis

The ADME and physicochemical properties of selected 5a, 5c, and Celecoxib were assessed through SwissADME (http://www.swissadme.ch/) webserver and these are presented in **Table 6**. From the assessed data in **Table 6**, the 5a, 5c, and Celecoxib was found not to violate Lipinski's rule of five. The polar surface area of test compound **5a** was 64.68 Å², **5c** was 90.70 Å² and Celecoxib 88.99Å². The findings also showed that the 5a, 5c, and Celecoxib had high human gastro intestinal (GI) absorption, In general, increased GI absorption leads to increased chemical bioavailability. As a result, oral administration of the test substance **5a, 5c** may result in improved absorption from the gastrointestinal system.

The higher numbers of H-bonds are possibly measured to be involved during protein ligand binding. From the result, the bioavailability score of three compounds showed better results +0.55 for **5a, 5c, and** Celecoxib. Thus relating with molecular properties 5a, 5c, and Celecoxib was predicted to have better chances as a possible drug-relevant candidate with antiinflammatory potential.

The test compounds and standard are soluble in nature, the synthetic accessibility score was found to be >6 for **5a** with 3.66, **5a** with 3.57, Celecoxib with 3.70, which indicated that the all the compounds are very feasible to synthesize.

The graphical representations of lipinski rule of selected compounds are presented in the **Figure 11**. The pink area within the hexagon represents the optimal range of the compounds. The recommended range for drug-like compound was in saturation (INSATU): fraction of carbons in the sp^3 hybridization not less than 0.25, insolubility (INSOLU): log S not higher than 6, hydrophobicity (LIPO): between -0.7 and +5.0, rotatable bonds (FLEXI): no more than 9 rotatable bonds, molecular weight (SIZE): between 150 and 500 g.mol^{-1}, polar surface area (POLAR): The red slanted hexagon inside the pink tint represents the reference compounds, which have drug-like characteristics. Based on the observation 5a, 5c, and Celecoxib had drug-like qualities.

Furthermore, the pharmacokinetic parameters of the chosen chemical, and standard, were studied using the egg-boiled model represented in **Figure 12**. Predicting passive gastrointestinal absorption and BBB penetration using the egg-boiled model is useful because it takes into account two important pharmacokinetic features at once. Egg-shaped plot demonstrates that chemical in yolk (i.e. yellow area) represents very possible BBB permeability and albumin (i.e. white region) represents highly probable human intestine absorption, as shown by the egg-shaped plot of organisational structure. From the **Figure 12**, the 5a, 5c, and Celecoxib found in albumin (white region) elucidated the good absorption in gastrointestinal region. From the above observed results, it can be interpreted that the **5a** and **5c** compounds have sufficient potential to be drug.

Synthesis of 1-(substitutedmethyl)indoline-2,3-dione (2a-2b)

A mixture of isatin (1.47 g; 0.01 mol), formaldehyde (0.45 g; 0.015 mol), and morpholine/piperidine (0.87/0.85 g; 0.01 mol) in ethanol (25 ml) was stirred for 2 h in magnetic stirrer. Then the resulting mixture was refluxed on water bath for 4 h. The above mixture was poured on crushed ice and mixed well. The solid **2a/2b** which obtained was filtered, dried, and recrystallised using rectified spirit.

1-(Morpholinomethyl)indoline-2,3-dione (2a)

Yield: 77 % (1.89 g), m.p.: 243-245 °C, R_f Value: 0.49 [Toluene: n-Propanol (40: 60)]. IR (KBr, cm^{-1}): 3094 (Ar-CH), 2937 (CH$_2$-CH), 1692 (C=O), 1613 (C=C), 1040 (C-O-C). ^{1}H NMR (CDCl$_3$, 500 MHz) δ ppm: 2.13-4.35 (m, 8H, CH$_2$ of

morpholine), 4.96 (s, 2H, CH$_2$ linkage), 7.28-7.90 (m, 4H, Ar-H). ^{13}C-NMR (δ: ppm): 51.7 (C-2' & C-6'), 63.2 (C-3' & C-5'), 74.5 (CH$_2$ linkage), 119.1 (C-8), 124.0 (C-7), 125.8 (C-5), 130.3 (C-4), 136.9 (C-6), 151.6 (C-9), 158.2 (C-2), 188.4 (C-3). EI-MS m/z: 246 (M$^+$). Anal. Cald for C$_{13}$H$_{14}$N$_2$O$_3$: C, 63.40; H, 5.73; N, 11.38. Found: C, 63.62; H, 5.71; N, 11.35.

1-(Piperidin-1-ylmethyl)indoline-2,3-dione (2b)

Yield: 73 % (1.78 g), m.p.: 219-221 °C, R$_f$ Value: 0.62 [Toluene: n-Propanol (40: 60)]. IR (KBr, cm^{-1}): 3069 (Ar-CH), 2922 (CH$_2$-CH), 1687 (C=O), 1591 (C=C). ^{1}H NMR (CDCl$_3$, 500 MHz) δ ppm: 1.87-2.99 (m, 10H, CH$_2$ of piperidine), 4.53 (s, 2H, CH$_2$ linkage), 7.02-7.97 (m, 4H, Ar-H). ^{13}C-NMR (δ: ppm): 24.7 (C-3' & C-5'), 25.1 (C-4'), 52.3 (C-2' & C-6'), 72.8 (CH$_2$ linkage), 118.0 (C-8), 123.3 (C-7), 125.2 (C-5), 128.6 (C-4), 133.5 (C-6), 148.9 (C-9), 159.3 (C-2), 185.0 (C-3). EI-MS m/z: 244 (M$^+$). Anal. Cald for C$_{14}$H$_{16}$N$_2$O$_2$: C, 68.83; H, 6.60; N, 11.47. Found: C, 69.06; H, 6.61; N, 11.43.

Synthesis of 4-(1-(substituted methyl)-2-oxoindolin-3-ylideneamino) benzoic acid (3a-3b)

Equimolar quantity of 1-(substitutedmethyl)indoline-2,3-dione **2a/2b** (2.46/2.44 g; 0.01 mol)and p-amino benzoic acid (1.37 g; 0.01 mol) in ethanol (30 ml) was refluxed on sand bath for 5 h. The reaction mixture was cooled to room temperature, poured in crushed ice and kept aside overnight in refrigerator. The product separated **3a/3b** was filtered, dried and recrystallised using ethanol.

4-(1-(Morpholinomethyl)-2-oxoindolin-3-ylideneamino)benzoic acid (3a)

Yield: 70 % (2.56 g), m.p.: 142-144 °C, R$_f$ Value: 0.35 [Toluene: n-Propanol (40: 60)]. IR (KBr, cm^{-1}): 3405 (OH), 3071 (Ar-CH), 2946 (CH$_2$-CH), 1729 (C=O), 1668 (C=N), 1594 (C=C), 1072 (C-O-C). ^{1}H NMR (CDCl$_3$, 500 MHz) δ ppm: 2.01-4.14 (m, 8H, CH$_2$ of morpholine), 4.48 (s, 2H, CH$_2$ linkage), 6.95-8.22 (m, 8H, Ar-H), 10.09 (s, 1H, OH). ^{13}C-NMR (δ: ppm): 50.8 (C-2' & C-6'), 65.1 (C-3' & C-5'), 72.0 (CH$_2$ linkage), 119.4 (C-8), 122.5 (C-7), 123.0 (C-2" & C-6"), 124.7 (C-5), 127.6 (C-4"), 129.1 (C-4), 132.3 (C-6), 132.9 (C-3" & C-5"), 150.2 (C-9), 157.5 (C-1"), 162.9 (C-3), 163.4 (C-2), 168.6 (COOH). EI-MS m/z: 365 (M$^+$). Anal. Cald for C$_{20}$H$_{19}$N$_3$O$_4$: C, 65.74; H, 5.24; N, 11.50. Found: C, 65.51; H, 5.26; N, 11.53.

4-(2-Oxo-1-(piperidin-1-ylmethyl)indolin-3-ylideneamino)benzoicacid (3b)

Yield: 78 % (2.83 g), m.p.: 130-132 °C, R$_f$ Value: 0.48 [Toluene: n-Propanol (40: 60)]. IR (KBr, cm^{-1}): 3422 (OH), 3058 (Ar-CH), 2910 (CH$_2$-CH), 1719 (C=O), 1681 (C=N), 1596 (C=C). ^{1}H NMR (CDCl$_3$, 500 MHz) δ ppm: 1.95-3.27 (m, 10H, CH$_2$ of piperidine), 4.32 (s, 2H, CH$_2$ linkage), 7.11-8.38 (m, 8H, Ar-H), 9.94 (s, 1H, OH). ^{13}C-NMR (δ: ppm): 26.0 (C-3' & C-5'), 26.4 (C-4'), 52.7 (C-2' & C-6'), 69.8 (CH$_2$ linkage), 115.2 (C-8), 121.6 (C-7), 122.9 (C-2" & C-6"), 123.4 (C-5), 130.1 (C-4"), 130.8 (C-4), 132.6 (C-6), 133.0 (C-3" & C-5"), 149.5 (C-9), 156.2 (C-1"), 164.6 (C-3), 164.9 (C-2), 170.3 (COOH). EI-MS m/z: 363 (M$^+$). Anal. Cald for C$_{21}$H$_{21}$N$_3$O$_3$: C, 69.41; H, 5.82; N, 11.56. Found: C, 69.62; H, 5.81; N, 11.54.

Synthesis of 4-(1-(substitutedmethyl)-2-oxoindolin-3-ylideneamino) benzohydrazide (4a-4b)

To 4-(1-(substitutedmethyl)-2-oxoindolin-3-ylideneamino)benzoicacid **3a/3b** (3.65/3.63 g; 0.01 mol), thionyl chloride (1.78 g; 0.015 mol) was added slowly with stirring and refluxed gently for 2 h. The excess of thionyl chloride was distilled off, and the reaction mixture was cooled in ice bath. The product thus formed was immediately used for next step. To the above product, ethanol (50 ml) was added. To this solution 95 % hydrazine hydrate (1 g; 0.02 mol) was slowly added with stirring. Then the mixture was refluxed for 10 h followed by removal of excess solvent under reduced pressure, and resultant solution was poured in ice cold water. The product separated **4a/4b** was filtered, and recrystallised from ethanol.

4-(1-(morpholinomethyl)-2-oxoindolin-3-ylideneamino)benzohydrazide (4a)

Yield: 72 % (2.73 g), m.p.: 166-168 °C, R_f Value: 0.76 [Hexane: Chloroform: n-Butanol (20: 30: 50)]. IR (KBr, cm^{-1}): 3347 & 3283 (NH), 3075 (Ar-CH), 2920 (CH$_2$-CH), 1681 (C=O), 1657 (C=N), 1589 (C=C), 1056 (C-O-C). ^{1}H NMR (CDCl$_3$, 500 MHz) δ ppm: 2.70-4.29 (m, 8H, CH$_2$ of morpholine), 4.55 (s, 2H, CH$_2$ linkage), 5.23 (s, 2H, NH$_2$), 6.86-8.12 (m, 8H, Ar-H), 8.61 (s, 1H, NH of hydrazide). ^{13}C-NMR (δ: ppm): 51.5 (C-2' & C-6'), 67.9 (C-3' & C-5'), 71.3 (CH$_2$ linkage), 116.1 (C-8), 120.6 (C-7), 123.2 (C-2" & C-6"), 124.4 (C-5), 127.5 (C-3" & C-5"), 128.0 (C-4), 130.8 (C-6), 134.8 (C-4"), 145.6 (C-9), 155.3 (C-1"), 161.8 (C-3), 162.1 (C-2), 163.5 (CONHNH$_2$). EI-MS m/z: 379 (M$^+$). Anal. Cald for C$_{20}$H$_{21}$N$_5$O$_3$: C, 63.31; H, 5.58; N, 18.46. Found: C, 63.50; H, 5.57; N, 18.48.

4-(2-Oxo-1-(piperidin-1-ylmethyl)indolin-3-ylideneamino)benzo hydrazide (4b)

Yield: 75 % (2.83 g), m.p.: 181-183 °C, R_f Value: 0.60 [Hexane: Chloroform: n-Butanol (40: 20: 40)]. IR (KBr, cm^{-1}): 3362 & 3319 (NH), 3056 (Ar-CH), 2928 (CH$_2$-CH), 1674 (C=O), 1641 (C=N), 1604 (C=C). ^{1}H NMR (CDCl$_3$, 500 MHz) δ ppm: 1.73-2.96 (m, 10H, CH$_2$ of piperidine), 4.62 (s, 2H, CH$_2$ linkage), 5.08 (s, 2H, NH$_2$), 7.25-8.31 (m, 8H, Ar-H), 8.94 (s, 1H, NH of hydrazide). ^{13}C-NMR (δ: ppm): 25.4 (C-3' & C-5'), 25.9 (C-4'), 52.1 (C-2' & C-6'), 72.5 (CH$_2$ linkage), 117.6 (C-8), 121.3 (C-7), 123.8 (C-2" & C-6"), 125.2 (C-5), 128.2 (C-3" & C-5"), 130.7 (C-4), 132.4 (C-6), 133.5 (C-4"), 146.8 (C-9), 154.0 (C-1"), 164.2 (C-3), 164.8 (C-2), 165.3 (CONHNH$_2$). EI-MS m/z: 377 (M$^+$). Anal. Cald for C$_{21}$H$_{23}$N$_5$O$_2$: C, 66.83; H, 6.14; N, 18.55. Found: C, 66.64; H, 6.16; N, 18.52.

Synthesis of 3-(4-(5-(substituted phenyl)-3-phenyl-4,5-dihydro-1H-pyrazole-1-carbonyl) phenylimino)-1-(substitutedmethyl)indolin-2-one (5a-5l)

Equimolar quantity of various aromatic/heterocyclic aldehydes (0.01 mol) and acetophenone (1.20 g; 0.01 mol) was dissolved in minimum quantity of ethanol. To this mixture, a catalytic quantity of sodium hydroxide pellet was added. Then the reaction mixture was stirred for 2-8 h and poured on ice cold water. The product separated (chalcone) was filtered, dried and utilized for further step. Various aromatic chalcone (0.01 mol) was added to the 4-(1-(substitutedmethyl)-2-oxoindolin-3-ylideneamino)benzohydrazide **4a/4b** (3.79/3.77 g; 0.01 mol) in round bottom flask containing *N,N*-dimethyl formamide (50 ml). The above mixture was refluxed in oil bath for a period of 12 h. Then the reaction mixture was cooled, poured in to a beaker containing ice cold water, and kept aside for 24 h. The obtained product **5a-5l** was separated by filtration, dried over the filter paper, and recrystallised using ethanol.

3-(4-(5-(4-Chlorophenyl)-3-phenyl-4,5-dihydro-1*H*-pyrazole-1-carbonyl) phenylimino)-1-(morpholinomethyl)indolin-2-one (5a)

Yield: 71 % (4.28 g), m.p.: 265-267 °C, R_f Value: 0.51 [Hexane: Chloroform: n-Butanol (20: 30: 50)]. IR (KBr, cm^{-1}): 3024 (Ar-CH), 2971 (CH$_2$-CH), 1740 (C=O), 1677 (C=N), 1591 (C=C), 1029 (C-O-C), 756(C-Cl). ^{1}H NMR (CDCl$_3$, 500 MHz) δ ppm: 1.84 (d, 2H, CH$_2$ of pyrazole), 2.31-2.87 (m, 8H, CH$_2$ of morpholine), 4.26 (s, 2H, CH$_2$ linkage), 5.14 (t, 1H, CH of pyrazole), 6.93-8.25 (m, 17H, Ar-H). ^{13}C-NMR (δ: ppm): 38.4 (CH$_2$ of pyrazole), 52.6 (C-2' & C-6'), 59.5 (C-5 of pyrazole), 65.8 (C-3' & C-5'), 70.6 (CH$_2$ linkage), 115.2 (C-8), 122.3 (C-7), 123.0 (C-2" & C-6"), 125.9 (C-5), 130.7 (C-2''' & C-6'''), 130.9 (C-3''' & C-5'''), 131.0 (C-3" & C-5"), 131.3 (C-3'''' & C-5''''), 131.9 (C-2'''' & C-6''''), 132.1 (C-4), 132.5 (C-4'''), 133.0 (C-6), 133.2 (C-4'''), 134.5 (C-4"), 135.7 (C-1''''), 140.2 (C-1'''), 146.4 (C-9), 150.4 (C-3 of pyrazole), 154.6 (C-1"), 166.2 (C-3), 166.1 (C-2), 170.8 (CO). EI-MS m/z: 603 (M$^+$), 605 (M^{+2}). Anal. Cald for C$_{35}$H$_{30}$ClN$_5$O$_3$: C, 69.59; H, 5.01; N, 11.59. Found: C, 70.25; H, 4.99; N, 11.56.

1-(Morpholinomethyl)-3-(4-(3-phenyl-5-(4-(trifluoromethyl)phenyl)-4,5-dihydro-1*H*-pyrazole-1-carbonyl)phenylimino)indolin-2-one (5b)

Yield: 79 % (5.03 g), m.p.: 209-212 °C, R_f Value: 0.84 [Hexane: Chloroform: n-Butanol (20: 30: 50)]. IR (KBr, cm^{-1}): 3072 (Ar-CH), 2939 (CH$_2$-CH), 1681 (C=O), 1654 (C=N), 1596 (C=C), 1135 (C-O-C), 1127(C-F). ^{1}H NMR (CDCl$_3$, 500 MHz) δ ppm: 1.87 (d, 2H, CH$_2$ of pyrazole), 2.52-3.04 (m, 8H, CH$_2$ of morpholine), 4.11 (s, 2H, CH$_2$ linkage), 5.08 (t, 1H, CH of pyrazole), 7.13-8.22 (m, 17H, Ar-H). ^{13}C-NMR (δ: ppm): 40.1 (CH$_2$ of pyrazole), 50.6 (C-2' & C-6'), 60.2 (C-5 of pyrazole), 64.5 (C-3' & C-5'), 71.0 (CH$_2$ linkage), 116.2 (C-8), 120.8 (C-7), 121.0 (C-2'' & C-6''), 125.3 (CF$_3$), 125.8 (C-5), 126.0 (C-3''' & C-5'''), 127.4 (C-2''' & C-6'''), 129.3 (C-3'' & C-5''), 129.6 (C-3'''' & C-5''''), 129.8 (C-2'''' & C-6''''), 130.1 (C-4), 130.4 (C-4''''), 131.2 (C-6), 129.5 (C-4''), 133.9 (C-4''), 135.3 (C-1''''), 145.1 (C-1'''), 148.7 (C-9), 153.1 (C-3 of pyrazole), 156.8 (C-1''), 165.0 (C-3), 165.4 (C-2), 169.5 (CO). EI-MS *m/z*: 637 (M$^+$). Anal. Cald for C$_{36}$H$_{30}$F$_3$N$_5$O$_3$: C, 67.81; H, 4.74; N, 10.98. Found: C, 67.63; H, 4.73; N, 11.02.

1-(Morpholinomethyl)-3-(4-(5-(4-nitrophenyl)-3-phenyl-4,5-dihydro-1*H*-pyrazole-1-carbonyl)phenylimino)indolin-2-one (5c)

Yield: 76 % (4.67 g), m.p.: 234-236 °C, R_f Value: 0.47 [Hexane: Chloroform: n-Butanol (20: 30: 50)]. IR (KBr, cm^{-1}): 3056 (Ar-CH), 2943 (CH$_2$-CH), 1687 (C=O), 1642 (C=N), 1588 (C=C), 1550 & 1321 (NO$_2$), 1119 (C-O-C). ^{1}H NMR (CDCl$_3$, 500 MHz) δ ppm: 2.10 (d, 2H, CH$_2$ of pyrazole), 2.44-2.91 (m, 8H, CH$_2$ of morpholine), 4.23 (s, 2H, CH$_2$ linkage), 5.25 (t, 1H, CH of pyrazole), 7.09-8.07 (m, 17H, Ar-H). ^{13}C-NMR (δ: ppm): 37.3 (CH$_2$ of pyrazole), 50.2 (C-2' & C-6'), 57.7 (C-5 of pyrazole), 67.6 (C-3' & C-5'), 69.3 (CH$_2$ linkage), 118.5 (C-8), 120.1 (C-3''' & C-5'''), 121.9 (C-7), 123.6 (C-2'' & C-6''), 125.4 (C-5), 127.0 (C-2''' & C-6'''), 129.4 (C-3'' & C-5''), 129.7 (C-3'''' & C-5''''), 130.4 (C-2'''' & C-6''''), 131.0 (C-4), 132.9 (C-4''''), 133.5 (C-6), 133.6 (C-4''), 135.2 (C-1''''), 146.8 (C-4'''), 149.3 (C-9), 151.8 (C-1''), 152.3 (C-3 of pyrazole), 159.4 (C-1''), 164.5 (C-3), 165.6 (C-2), 168.0 (CO). EI-MS *m/z*: 614 (M$^+$). Anal. Cald for C$_{35}$H$_{30}$N$_6$O$_5$: C, 68.39; H, 4.92; N, 13.67. Found: C, 68.53; H, 4.93; N, 13.64.

1-(Morpholinomethyl)-3-(4-(3-phenyl-5-p-tolyl-4,5-dihydro-1*H*-pyrazole-1-carbonyl) phenylimino)indolin-2-one (5d)

Yield: 73 % (4.26 g), m.p.: 250-252 °C, R_f Value: 0.55 [Hexane: Chloroform: n-Butanol (20: 30: 50)]. IR (KBr, cm^{-1}): 3068 (Ar-CH), 2951 (CH$_2$-CH), 1665 (C=O), 1647 (C=N), 1594 (C=C), 1120 (C-O-C). ^{1}H NMR (CDCl$_3$, 500 MHz) δ ppm: 1.83 (d, 2H, CH$_2$ of pyrazole), 2.12 (s, 3H, CH$_3$), 2.58-3.16 (m, 8H, CH$_2$ of morpholine), 4.30 (s, 2H, CH$_2$ linkage), 5.09 (t, 1H, CH of pyrazole), 6.84-7.91 (m, 17H, Ar-H). ^{13}C-NMR (δ: ppm): 26.7 (CH$_3$), 39.4 (CH$_2$ of pyrazole), 49.7 (C-2' & C-6'), 56.1 (C-5 of pyrazole), 65.0 (C-3' & C-5'), 73.9 (CH$_2$ linkage), 114.5 (C-8), 118.2 (C-7), 120.8 (C-2'' & C-6''), 123.6 (C-5), 126.3 (C-2''' & C-6'''), 128.1 (C-3'' & C-5''), 127.5 (C-3'' & C-5''), 127.7 (C-3'''' & C-5''''), 129.0 (C-2'''' & C-6''''), 129.2 (C-4), 130.3 (C-4''''), 132.6 (C-6), 135.9 (C-4'''), 133.4 (C-4''), 133.8 (C-1''''), 142.7 (C-1'''), 147.5 (C-9), 150.6 (C-3 of pyrazole), 158.1 (C-1''), 162.9 (C-3), 163.8 (C-2), 167.3 (CO). EI-MS *m/z*: 583 (M$^+$). Anal. Cald for C$_{36}$H$_{33}$N$_5$O$_3$: C, 74.08; H, 5.70; N, 12.00. Found: C, 74.26; H, 5.68; N, 11.97.

3-(4-(5-(4-Aminophenyl)-3-phenyl-4,5-dihydro-1*H*-pyrazole-1-carbonyl)phenylimino)-1-(morpholinomethyl)indolin-2-one (5e)

Yield: 78 % (4.56 g), m.p.: 197-199 °C, R_f Value: 0.42 [Hexane: Chloroform: n-Butanol (20: 30: 50)]. IR (KBr, cm^{-1}): 3301 (NH), 3023 (Ar-CH), 2946 (CH$_2$-CH), 1740 (C=O), 1668 (C=N), 1631 (C=C), 1110 (C-O-C). ^{1}H NMR (CDCl$_3$, 500 MHz) δ ppm: 1.91 (d, 2H, CH$_2$ of pyrazole), 2.70-3.23 (m, 8H, CH$_2$ of morpholine), 4.02 (s, 2H, NH$_2$), 4.63 (s, 2H, CH$_2$ linkage),

5.49 (t, 1H, CH of pyrazole), 7.21-8.68 (m, 17H, Ar-H). ^{13}C-NMR (δ: ppm): 39.7 (CH$_2$ of pyrazole), 51.3 (C-2' & C-6'), 60.8 (C-5 of pyrazole), 66.1 (C-3' & C-5'), 72.4 (CH$_2$ linkage), 114.3 (C-3''' & C-5'''), 117.8 (C-8), 119.5 (C-7), 120.4 (C-2'' & C-6''), 123.0 (C-5), 126.7 (C-2'' & C-6''), 129.5 (C-3'' & C-5''), 130.2 (C-3''' & C-5'''), 130.6 (C-2'''' & C-6''''), 130.9 (C-4), 132.4 (C-4''''), 132.8 (C-6), 133.1 (C-4''), 134.0 (C-1'''), 135.6 (C-1''''), 144.3 (C-4'''), 148.9 (C-9), 151.9 (C-3 of pyrazole), 156.1 (C-1''), 161.3 (C-3), 161.4 (C-2), 166.2 (CO). EI-MS m/z: 584 (M$^+$). Anal. Cald for C$_{35}$H$_{32}$N$_6$O$_3$: C, 71.90; H, 5.52; N, 14.37. Found: C, 71.68; H, 5.54; N, 14.41.

3-(4-(5-(4-Hydroxyphenyl)-3-phenyl-4,5-dihydro-1H-pyrazole-1-carbonyl)phenylimino)-1-(morpholinomethyl)indolin-2-one (5f)

Yield: 80 % (4.68 g), m.p.: 228-230 °C, R$_f$ Value: 0.69 [Hexane: Chloroform: n-Butanol (20: 30: 50)]. IR (KBr, cm^{-1}): 3557 (OH), 3040 (Ar-CH), 2934 (CH$_2$-CH), 1679 (C=O), 1665 (C=N), 1599 (C=C), 1136 (C=O). ^{1}H NMR (CDCl$_3$, 500 MHz) δ ppm: 1.86 (d, 2H, CH$_2$ of pyrazole), 2.49-3.03 (m, 8H, CH$_2$ of morpholine), 4.25 (s, 2H, CH$_2$ linkage), 5.24 (t, 1H, CH of pyrazole), 5.61 (s, 1H, OH), 7.01-8.37 (m, 17H, Ar-H). ^{13}C-NMR (δ: ppm): 37.2 (CH$_2$ of pyrazole), 54.9 (C-2' & C-6'), 57.0 (C-5 of pyrazole), 68.3 (C-3' & C-5'), 70.5 (CH$_2$ linkage), 112.4 (C-3''' & C-5'''), 118.7 (C-8), 122.3 (C-7), 123.2 (C-2'' & C-6''), 126.1 (C-5), 130.6 (C-2'' & C-6''), 131.2 (C-3'' & C-5''), 132.5 (C-3''' & C-5'''), 132.8 (C-2'''' & C-6''''), 133.0 (C-4), 133.7 (C-4''''), 134.3 (C-6), 134.6 (C-4''), 135.4 (C-1''''), 137.1 (C-1'''), 149.0 (C-9), 152.5 (C-3 of pyrazole), 154.8 (C-4'''), 155.9 (C-1''), 163.1 (C-3), 164.0 (C-2), 168.6 (CO). EI-MS m/z: 585 (M$^+$). Anal. Cald for C$_{35}$H$_{31}$N$_5$O$_4$: C, 71.78; H, 5.34; N, 11.96. Found: C, 71.56; H, 5.35; N, 11.99.

3-(4-(5-(4-Chlorophenyl)-3-phenyl-4,5-dihydro-1H-pyrazole-1-carbonyl)phenylimino)-1-(piperidin-1-ylmethyl)indolin-2-one (5g)

Yield: 75 % (4.51 g), m.p.: 293-295 °C, R$_f$ Value: 0.53 [Hexane: Chloroform: n-Butanol (40: 20: 40)]. IR (KBr, cm^{-1}): 3076 (Ar-CH), 2957 (CH$_2$-CH), 1683 (C=O), 1658 (C=N), 1570 (C=C), 735 (C-Cl). ^{1}H NMR (CDCl$_3$, 500 MHz) δ ppm: 1.92 (d, 2H, CH$_2$ of pyrazole), 2.57-3.39 (m, 10H, CH$_2$ of piperidine), 4.26 (s, 2H, CH$_2$ linkage), 5.31 (t, 1H, CH of pyrazole), 7.25-8.10 (m, 17H, Ar-H). ^{13}C-NMR (δ: ppm): 24.9 (C-3' & C-5'), 25.3 (C-4'), 38.1 (CH$_2$ of pyrazole), 53.9 (C-2' & C-6'), 58.4 (C-5 of pyrazole), 71.7 (CH$_2$ linkage), 115.3 (C-8), 120.5 (C-7), 121.9 (C-2'' & C-6''), 124.5 (C-5), 127.2 (C-2'' & C-6''), 129.0 (C-3''' & C-5'''), 129.8 (C-3'' & C-5''), 130.0 (C-3'''' & C-5''''), 130.7 (C-2'''' & C-6''''), 131.0 (C-4), 131.1 (C-4''''), 131.4 (C-6), 133.5 (C-4''), 133.9 (C-4'''), 136.2 (C-1''''), 143.4 (C-1'''), 147.6 (C-9), 150.7 (C-3 of pyrazole), 157.0 (C-1''), 162.3 (C-3), 162.7 (C-2), 168.9 (CO). EI-MS m/z: 601 (M$^+$), 603 (M^{+2}). Anal. Cald for C$_{36}$H$_{32}$ClN$_5$O$_2$: C, 71.81; H, 5.36; N, 11.63. Found: C, 72.04; H, 5.34; N, 11.59.

3-(4-(3-Phenyl-5-(4-(trifluoromethyl)phenyl)-4,5-dihydro-1H-pyrazole-1-carbonyl) phenylimino)-1-(piperidin-1-ylmethyl)indolin-2-one (5h)

Yield: 72 % (4.57 g), m.p.: 152-154 °C, R$_f$ Value: 0.45 [Hexane: Chloroform: n-Butanol (40: 20: 40)]. IR (KBr, cm^{-1}): 3059 (Ar-CH), 2946 (CH$_2$-CH), 1678 (C=O), 1641 (C=N), 1585 (C=C), 1142 (C-F). ^{1}H NMR (CDCl$_3$, 500 MHz) δ ppm: 2.09 (d, 2H, CH$_2$ of pyrazole), 2.51-3.48 (m, 10H, CH$_2$ of piperidine), 4.12 (s, 2H, CH$_2$ linkage), 5.17 (t, 1H, CH of pyrazole), 7.05-8.25 (m, 17H, Ar-H). ^{13}C-NMR (δ: ppm): 23.2 (C-3' & C-5'), 23.6 (C-4'), 38.0 (CH$_2$ of pyrazole), 52.4 (C-2' & C-6'), 62.9 (C-5 of pyrazole), 69.8 (CH$_2$ linkage), 119.5 (C-8), 121.8 (C-7), 122.1 (C-2'' & C-6''), 123.0 (CF$_3$), 123.5 (C-5), 127.2 (C-3''' & C-5'''), 129.7 (C-2'''' & C-6''''), 130.2 (C-3'' & C-5''), 130.4 (C-3'''' & C-5''''), 130.5 (C-4''''), 131.3 (C-2'''' & C-6''''), 132.1 (C-4), 133.3 (C-4''''), 133.6 (C-6), 134.0 (C-4''), 135.5 (C-1''''), 148.7 (C-1''), 151.5 (C-9), 154.8 (C-3 of pyrazole),

157.5 (C-1″), 161.2 (C-3), 161.8 (C-2), 168.4 (CO). EI-MS m/z: 635 (M$^+$). Anal. Cald for $C_{37}H_{32}F_3N_5O_2$: C, 69.91; H, 5.07; N, 11.02. Found: C, 69.73; H, 5.09; N, 11.05.

3-(4-(5-(4-Nitrophenyl)-3-phenyl-4,5-dihydro-1*H*-pyrazole-1-carbonyl)phenylimino)-1-(piperidin-1-ylmethyl)indolin-2-one (5i)

Yield: 77 % (4.71 g), m.p.: 190-192 °C, R_f Value: 0.71 [Hexane: Chloroform: n-Butanol (40: 20: 40)]. IR (KBr, cm^{-1}): 3071 (Ar-CH), 2948 (CH$_2$-CH), 1674 (C=O), 1649 (C=N), 1582 (C=C), 1538 & 1343 (NO$_2$). ^{1}H NMR (CDCl$_3$, 500 MHz) δ ppm: 1.98 (d, 2H, CH$_2$ of pyrazole), 2.65-3.29 (m, 10H, CH$_2$ of piperidine), 4.36 (s, 2H, CH$_2$ linkage), 5.22 (t, 1H, CH of pyrazole), 6.90-8.04 (m, 17H, Ar-H). ^{13}C-NMR (δ: ppm): 25.8 (C-3' & C-5'), 25.9 (C-4'), 40.7 (CH$_2$ of pyrazole), 50.1 (C-2' & C-6'), 61.4 (C-5 of pyrazole), 68.4 (CH$_2$ linkage), 117.0 (C-8), 120.5 (C-3‴ & C-5‴), 122.6 (C-7), 124.3 (C-2″ & C-6″), 126.2 (C-5), 127.5 (C-2‴ & C-6‴), 128.3 (C-3″ & C-5″), 128.7 (C-3⁗ & C-5⁗), 129.8 (C-2⁗ & C-6⁗), 130.2 (C-4), 130.9 (C-4⁗), 131.7 (C-6), 134.1 (C-4″), 136.0 (C-1⁗), 145.2 (C-4‴), 150.9 (C-9), 151.5 (C-1‴), 153.4 (C-3 of pyrazole), 154.9 (C-1″), 165.0 (C-3), 165.3 (C-2), 170.7 (CO). EI-MS m/z: 612 (M$^+$). Anal. Cald for $C_{36}H_{32}N_6O_4$: C, 70.57; H, 5.26; N, 13.72. Found: C, 70.78; H, 5.27; N, 13.69.

3-(4-(3-Phenyl-5-p-tolyl-4,5-dihydro-1*H*-pyrazole-1-carbonyl) phenylimino)-1-(piperidin-1-ylmethyl)indolin-2-one (5j)

Yield: 74 % (4.30 g), m.p.: 281-284 °C, R_f Value: 0.49 [Hexane: Chloroform: n-Butanol (40: 20: 40)]. IR (KBr, cm^{-1}): 3015 (Ar-CH), 2952 (CH$_2$-CH), 1666 (C=O), 1643 (C=N), 1597 (C=C). ^{1}H NMR (CDCl$_3$, 500 MHz) δ ppm: 1.80 (d, 2H, CH$_2$ of pyrazole), 2.28 (s, 3H, CH$_3$), 2.46-3.02 (m, 10H, CH$_2$ of piperidine), 4.14 (s, 2H, CH$_2$ linkage), 5.27 (t, 1H, CH of pyrazole), 7.11-8.36 (m, 17H, Ar-H). ^{13}C-NMR (δ: ppm): 22.4 (CH$_3$), 23.7 (C-3' & C-5'), 24.0 (C-4'), 41.9 (CH$_2$ of pyrazole), 51.5 (C-2' & C-6'), 58.6 (C-5 of pyrazole), 73.2 (CH$_2$ linkage), 117.5 (C-8), 120.4 (C-7), 123.8 (C-2″ & C-6″), 125.3 (C-5), 126.1 (C-2‴ & C-6‴), 127.5 (C-3‴ & C-5‴), 127.8 (C-3″ & C-5″), 128.0 (C-3⁗ & C-5⁗), 128.6 (C-2⁗ & C-6⁗), 129.2 (C-4), 129.7 (C-4⁗), 131.5 (C-6), 132.4 (C-4″), 135.1 (C-1⁗), 136.8 (C-4‴), 143.4 (C-1‴), 148.6 (C-9), 149.2 (C-3 of pyrazole), 156.7 (C-1″), 164.5 (C-3), 164.7 (C-2), 167.9 (CO). EI-MS m/z: 581 (M$^+$). Anal. Cald for $C_{37}H_{35}N_5O_2$: C, 76.40; H, 6.06; N, 12.04. Found: C, 76.25; H, 6.08; N, 12.03.

3-(4-(5-(4-Aminophenyl)-3-phenyl-4,5-dihydro-1*H*-pyrazole-1-carbonyl) phenylimino)-1-(piperidin-1-ylmethyl)indolin-2-one (5k)

Yield: 71 % (4.13 g), m.p.: 257-259 °C, R_f Value: 0.80 [Hexane: Chloroform: n-Butanol (40: 20: 40)]. IR (KBr, cm^{-1}): 3324 (NH), 3067 (Ar-CH), 2935 (CH$_2$-CH), 1682 (C=O), 1676 (C=N), 1573 (C=C). ^{1}H NMR (CDCl$_3$, 500 MHz) δ ppm: 1.95 (d, 2H, CH$_2$ of pyrazole), 2.53-3.35 (m, 10H, CH$_2$ of piperidine), 3.97 (s, 2H, NH$_2$), 4.28 (s, 2H, CH$_2$ linkage), 5.36 (t, 1H, CH of pyrazole), 6.82-8.13 (m, 17H, Ar-H). ^{13}C-NMR (δ: ppm): 26.5 (C-3' & C-5'), 27.1 (C-4'), 39.7 (CH$_2$ of pyrazole), 51.3 (C-2' & C-6'), 59.0 (C-5 of pyrazole), 70.7 (CH$_2$ linkage), 113.2 (C-3‴ & C-5‴), 119.2 (C-8), 120.9 (C-7), 121.4 (C-2″ & C-6″), 124.9 (C-5), 126.7 (C-2‴ & C-6‴), 127.6 (C-3″ & C-5″), 127.8 (C-3⁗ & C-5⁗), 128.1 (C-2⁗ & C-6⁗), 128.6 (C-4), 128.9 (C-4⁗), 129.3 (C-6), 131.7 (C-4″), 132.5 (C-1‴), 133.4 (C-1⁗), 147.1 (C-4‴), 151.9 (C-9), 152.5 (C-3 of pyrazole), 157.3 (C-1″), 161.0 (C-3), 162.7 (C-2), 168.1 (CO). EI-MS m/z: 582 (M$^+$). Anal. Cald for $C_{36}H_{34}N_6O_2$: C, 74.20; H, 5.88; N, 14.42. Found: C, 74.03; H, 5.86; N, 14.47.

3-(4-(5-(4-Hydroxyphenyl)-3-phenyl-4,5-dihydro-1*H*-pyrazole-1-carbonyl)phenylimino)-1-(piperidin-1-ylmethyl)indolin-2-one (5l)

Yield: 76 % (4.43 g), m.p.: 222-224 °C, R_f Value: 0.38 [Hexane: Chloroform: n-Butanol (40: 20: 40)]. IR (KBr, cm^{-1}): 3528 (OH), 3023 (Ar-CH), 2947 (CH$_2$-CH), 1740 (C=O), 1667 (C=N), 1629 (C=C). ^{1}H NMR (CDCl$_3$, 500 MHz) δ ppm: 2.01 (d, 2H, CH$_2$ of pyrazole), 2.61-3.27 (m, 10H, CH$_2$ of piperidine), 4.11 (s, 2H, CH$_2$ linkage), 4.70 (t, 1H, CH of pyrazole), 5.31 (s, 1H, OH), 7.01-8.54 (m, 17H, Ar-H). ^{13}C-NMR (δ: ppm): 24.1 (C-3' & C-5'), 24.5 (C-4'), 42.6 (CH$_2$ of pyrazole), 50.7 (C-2' & C-6'), 62.3 (C-5 of pyrazole), 71.4 (CH$_2$ linkage), 114.7 (C-3''' & C-5'''), 116.3 (C-8), 121.9 (C-7), 122.9 (C-2'' & C-6''), 126.2 (C-5), 129.8 (C-2''' & C-6'''), 130.0 (C-3'' & C-5''), 130.1 (C-3'''' & C-5''''), 130.9 (C-2'''' & C-6''''), 131.5 (C-4), 131.8 (C-4''''), 132.4 (C-6), 133.6 (C-4''), 134.9 (C-1''''), 139.5 (C-1'''), 150.2 (C-9), 151.4 (C-3 of pyrazole), 154.3 (C-4'''), 155.2 (C-1''), 162.7 (C-3), 163.1 (C-2), 166.8 (CO). EI-MS m/z: 583 (M$^+$). Anal. Cald for C$_{36}$H$_{33}$N$_5$O$_3$: C, 74.08; H, 5.70; N, 12.00. Found: C, 74.36; H, 5.71; N, 11.96.

CHEMISTRY

A range of novel pyrazole substituted isatin derivatives were synthesized by multistep synthesis from indole-2,3-dione in the present study. Initially, isatin **1** was treated with morpholine/piperidine and formaldehyde to produce 1-(substitutedmethyl)indoline-2,3-dione **2a-2b** by Mannich reaction. In the succeeding stair, 4-(1-(substitutedmethyl)-2-oxoindolin-3-ylideneamino)benzoic acid **3a-3b** was synthesized through the condensation of compound **2a-2b** with *p*-aminobenzoic acid in ethanol by Schiff base reaction. On treating with thionyl chloride followed by hydrazine hydrate, compounds **3a-3b** converted to its respective hydrazide derivatives [4-(1-(substitutedmethyl)-2-oxoindolin-3-ylideneamino)benzohydrazide] **4a-4b**. In the final step, the title compounds **5a-5l** were synthesized by a ring closure reaction, in which a different chalcones (α,β-unsaturated carbonyl compound) and hydrazide derivative of isatin derivatives **4a-4b** were reacted. TLC was performed throughout the reactions to optimize the reactions for purity and completion.

IR, ^{1}H-NMR, Mass spectra, and elemental analyses of the synthesized compounds are in accordance with the assigned structures. The IR spectra of all synthesized compounds showed some characteristic peaks indicating the presence of particular groups. Formation of the methylene linkage in compound **2a/2b** was confirmed by its absorption peak at 2937/2922 cm^{-1} in IR corresponds to CH$_2$-CH stretching respectively. This was further confirmed by appearance of singlet for two protons of CH$_2$ linkage at δ 4.96 and 4.53 ppm for compound **2a** and **2b** respectively. The absorption bands at 3405-3422 and 1668-1681cm^{-1}, which can be assignable to OH of COOH and C=N (azomethine linkage) vibrations respectively confirms the formation of compounds **3a-3b**. Appearance of singlet at δ 9.94-10.09 ppm for single protons in its ^{1}H-NMR spectra which might be assigned to OH of COOH group additionally support the structure of compounds **3a-3b**. The conversion of hydrazide **4a-4b** from carboxylic acid **3a-3b** can be recognized by strong absorption peak at 3283-3362 cm^{-1} in IR due to N-H stretching and appearance of singlet in its ^{1}H-NMR spectra at δ 5.08-5.23 ppm for two protons which might be assigned to NH$_2$ of hydrazide group. Presence of NH in hydrazide was confirmed by appearance of singlet for single proton in ^{1}H-NMR spectra at δ 8.61-8.94 ppm. The structure of title compounds **5a-5l** was confirmed by the absence of absorption band around 3300 cm^{-1} due to absence of NH stretching vibration. In addition appearance of doublet for two protons of C-4 pyrazole at δ 1.80-2.10 ppm and triplet for one proton of C-5 pyrazole at δ 4.70-5.49 ppm also confirms the structure of title compounds **5a-5l**. The IR spectrum of title compounds **5a-5l** shows absorption bands at 3015-3076 cm^{-1}, 2934-2971 cm^{-1}, 1665-1740 cm^{-1}, 1641-1677 cm^{-1} and 1570-1631 cm^{-1}, which can be assignable to Ar-CH, CH$_2$-CH, C=O, C=N and C=C vibrations respectively. The following conclusions can be derived by comparing the NMR spectra of synthesized compounds **5a-5l**: a) A doublet at δ 1.80-2.10 ppm for CH$_2$ of pyrazole, b) A multiplet at δ 2.31-3.48 ppm for CH$_2$ of morpholine/piperidine, c) A singlet at δ 4.11-4.63 ppm for CH$_2$ linkage, d) A triplet at δ 4.70-5.49 ppm for CH of pyrazole, e) A multiplet at δ 6.82-8.68 ppm for Ar-H. Further mass spectrum confirmed their molecular weight.

Elemental analysis of all synthesized compounds was found to be within ± 0.4 % with respect to calculated value which confirmed the purity of synthesized compounds.

Conclusions

IR, ^{1}HNMR, and Mass spectral analyses were used to examine and characterize the 3-(4-(substitutedphenyl)-3-phenyl-4,5-dihydro-1H-pyrazole-1-carbonyl)phenylimino)-1-(substituted methyl)indolin-2-one (5a-5l). In the active region of the target protein CXCR6, 3-(4-(5-(4-Chlorophenyl)-3-phenyl-4,5-dihydro-1*H*-pyrazole-1-carbonyl) phenylimino)-1-(morpholino

methyl) indolin-2-one (**5a**) showed considerable binding affinity and higher amino acid interaction, as well as a superior docking score of -11.4 kcal mol-1 (PDB: 6KVA). 5a displayed persistent binding affinity with the target CXCR6 receptor, according to molecular dynamics analysis. Among the other compounds studied, the **5a** had the strongest anti-inflammatory properties that to the novel **5a** could be used as an anti-inflammatory agent.

Declarations

Acknowledgements

Availability of data and materials

Not applicable to this manuscript.

Funding

Author contribution

TP, SK, and GS conceived and designed research, with conceptual input from PP, SP, GM (4th Author), YM and NS (6th Author) performed research work and analyse the data. TP, SK, and GS wrote the paper.

Ethics approval and consent to participate

File number was mentioned in the manuscript

Consent for publication

Not applicable to this manuscript.

Competing interests

The authors declare no competing interests.

References

1. Milenkovic VM, Stanton EH, Nothdurfter C, Rupprecht R, Wetzel CH (2019) The role of chemokines in the pathophysiology of major depressive disorder. Int J Mol Sci 20(9):2283

2. Hughes CE, Nibbs RJ (2018) A guide to chemokines and their receptors. FEBS J 285(16):2944–2971

3. Shiro T, Fukaya T, Tobe M (2015) The chemistry and biological activity of heterocycle-fused quinolinone derivatives: A review. Eur J Med Chem 97:397–408

4. Fu D-J, Zhang S-Y, Liu Y-C, Zhang L, Liu J-J, Song J et al (2016) Design, synthesis and antiproliferative activity studies of novel dithiocarbamate–chalcone derivates. Bioorg Med Chem Lett 26(16):3918–3922

5. Fu D-J, Yang J-J, Li P, Hou Y-H, Huang S-N, Tippin MA et al (2018) Bioactive heterocycles containing a 3, 4, 5-trimethoxyphenyl fragment exerting potent antiproliferative activity through microtubule destabilization. Eur J Med Chem 157:50–61

6. Fu D-J, Zhang L, Song J, Mao R-W, Zhao R-H, Liu Y-C et al (2017) Design and synthesis of formononetin-dithiocarbamate hybrids that inhibit growth and migration of PC-3 cells via MAPK/Wnt signaling pathways. Eur J Med Chem 127:87–99

7. Fu D-J, Song J, Hou Y-H, Zhao R-H, Li J-H, Mao R-W et al (2017) Discovery of 5, 6-diaryl-1, 2, 4-triazines hybrids as potential apoptosis inducers. Eur J Med Chem 138:1076–1088

8. Fu D-J, Zhang S-Y, Liu Y-C, Yue X-X, Liu J-J, Song J et al (2016) Design, synthesis and antiproliferative activity studies of 1, 2, 3-triazole–chalcones. MedChemComm 7(8):1664–1671

9. Yadav M, Murumkar PR, Ghuge RB (2018) Vicinal Diaryl Substituted Heterocycles: A Gold Mine for the Discovery of Novel Therapeutic Agents. Elsevier

10. Saravanan G, Panneerselvam T, Alagarsamy V, Kunjiappan S, Parasuraman P, Murugan I et al (2018) Design, graph theoretical analysis, density functionality theories, Insilico modeling, synthesis, characterization and biological activities of novel thiazole fused quinazolinone derivatives. Drug Dev Res 79(6):260–274

11. Kalimuthu AK, Panneerselvam T, Pavadai P, Pandian SRK, Sundar K, Murugesan S et al (2021) Pharmacoinformatics-based investigation of bioactive compounds of Rasam (South Indian recipe) against human cancer. Sci Rep 11(1):1–19

12. Kunjiappan S, Sankaranarayanan M, Kumar BK, Pavadai P, Babkiewicz E, Maszczyk P et al (2020) Capsaicin-loaded solid lipid nanoparticles: Design, biodistribution, in silico modeling and in vitro cytotoxicity evaluation. Nanotechnology 32(9):095101

13. Kunjiappan S, Panneerselvam T, Govindaraj S, Parasuraman P, Baskararaj S, Sankaranarayanan M et al (2019) Design, in silico modelling, and functionality theory of novel folate receptor targeted rutin encapsulated folic acid conjugated keratin nanoparticles for effective cancer treatment. Anti-Cancer Agents in Medicinal Chemistry (Formerly Current Medicinal Chemistry-Anti-Cancer Agents). 19:1966–198216

14. Selvam TP, Karthick V, Kumar PV, Ali MA (2012) Synthesis and structure-activity relationship study of 2-(substituted benzylidene)-7-(4-fluorophenyl)-5-(furan-2-yl)-2H-thiazolo [3, 2-a] pyrimidin-3 (7H)-one derivatives as anticancer agents. Drug Discoveries & Therapeutics 6(4):198–204

Tables

Table 1. The results of network analysis with threshold parameter values

Label	Degree	Betweenness	Closeness	Eccentricity	EigenVector	Radiality	Stress
CXCR6/Chemokine	12	944.0443	0.007299	0.125	0.439326	9	2262
FGR	9	584.7075	0.006944	0.111111	0.373908	8.877193	1574
PIK3CA	9	722.8035	0.007874	0.142857	0.425905	9.175439	1824
PTK2	5	155.8221	0.005952	0.125	0.216215	8.684211	448
GNB5	5	525.3959	0.006803	0.166667	0.243112	8.824561	1544
CDC42	5	325.54	0.005025	0.125	0.01427	7.912281	598
AKT3	5	494	0.00625	0.111111	0.18449	8.596491	1004
HRAS	5	286.0268	0.006135	0.111111	0.226833	8.54386	874
RAC1	5	294.9494	0.005682	0.111111	0.043618	8.315789	564
PIK3R6	5	90.51833	0.005814	0.1	0.235612	8.385965	316
PLCB1	4	575.5103	0.005882	0.166667	0.071534	8.421053	1830
GNAI1	4	231.2901	0.006494	0.125	0.208358	8.701754	372
VAV3	4	468.9595	0.005682	0.111111	0.052148	8.315789	876
ITK	4	426.4313	0.006289	0.111111	0.206495	8.614035	852
PRKCB	4	474.3308	0.004878	0.142857	0.018399	7.807018	1402
PRKCZ	4	159.6648	0.00641	0.2	0.217477	8.894737	540
RASGRP2	3	152.3333	0.00495	0.142857	0.018248	7.859649	282
PTK2B	3	79.44365	0.005181	0.1	0.08669	8.245614	274
PREX1	3	267.0604	0.006897	0.2	0.135306	8.859649	458

Table 2. The docking score and amino acid interaction of **5a-5l**

Code	R	Score	Amino acid interaction	Amino acid interaction
5a	4-Cl	**-11.4**	ARG39[2.64 Å], ARG86[3.06 Å, 4.71Å], LEU87[3.14 Å], ARG88[3.96 Å], ASP90[4.05 Å], GLNP111[3.13 Å,11.72Å], VAL154[2.63 Å],THR155[3.68 Å],VAL156[2.10 Å]	**11**
5b	4-CF$_3$	-11.4	GLN1[3.12 Å], PRO46[3.15 Å], PHE106 [16.51 Å,3.15Å], GLY108[3.52 Å], GLN179[4.12 Å], SER180[3.78 Å], SER185[3.19 Å]	8
5c	**4-NO$_2$**	**-11**	GLN1[2.00 Å, 3.31 Å, 3.31 Å, 4.53 Å, 15.37 Å], PRO42[3.94 Å], GLU47[3.55 Å], LYS64[3.59 Å], TRP104[3.32 Å], VAL105[3.14 Å],PHE106[2.16 Å]	**11**
5d	4-CH$_3$	-10.7	GLN6[3.59 Å], ARG39[5.17 Å], ALA41[2.87 Å], GLY45[, 2.24 Å 2.97 Å], GLU47[3.19 Å , 3.84 Å], GLY108[3.33 Å]	8
5e	4-NH$_2$	-10.8	GLN44[2.39 Å, 2.39 Å, 3.51 Å], ASP90[4.75 Å], VAL154[3.88 Å], VAL169[3.84 Å], THR171[11.12 Å]	7
5f	4-OH	-11.1	ARG88[5.12 Å], PRO89[5.00 Å], ASP90[4.26 Å], GLY152[2.87 Å], ALA153[3.51 Å], THR171[3.80 Å]	6
5g	4-Cl	-10.8	GLN1 [2.05 Å, 3.69 Å], GLU47 [3.72 Å], LYS64 [4.59 Å, 5.06 Å], TRP104[3.64 Å], THR173[3.50 Å], ALA176[3.04 Å]	8
5h	4-CF$_3$	-11.2	GLN1[3.25 Å], ARG39[2.78 Å], GLN44[2.29 Å], GLY45[2.71 Å], GLU47[3.64 Å], ASP90[3.31 Å], GLP168[3.37 Å], SER180[2.67 Å]	8
5i	4-NO$_2$	-11	GLP40[2.49 Å, 3.93 Å], GLY43[4.18 Å, 3.71 Å], GLN44[2.45 Å], ASP93[3.65 Å], TYR96[1.88 Å]	7
5j	4-CH$_3$	-10.5	TRP158[1.26 Å], VAL165[1.93 Å], LYS166[3.67 Å], TYR184[5.48 Å]	4
5k	4-NH$_2$	-11.1	GLN44 [2.36 Å, 3.24 Å], GLU47[3.49 Å], ASP90[4.70 Å], VAL154[3.85 Å, 3.00 Å], VAL169[3.80 Å], THR171[11.18 Å]	8
5l	4-OH	-11.7	GLP40 [2.46 Å, 4.00 Å], GLY43[3.78 Å], GLN44[2.62 Å], ASP93[3.57 Å],VAL94[3.81 Å], TYR96[1.97 Å], LYS166[2.29 Å]	8
Acetaminophen		-7.5	HSD100[2.21 Å], VAL119[2.88 Å], SER121[1.96 Å]	3
Celecoxib		-8.8	GLN1[4.16 Å], LEU4[3.03 Å], GLU47[4.26 Å,4.26 Å], TRP48[2.25 Å], TRP104[1.95 Å], PHE106[3.04 Å, 3.80 Å, 2.99 Å], GLY108[2.89 Å], SER180[2.97 Å]	11
Diclofenac		-7.4	ALA2[3.28 Å], PRO46[4.07 Å], TRP48[2.11 Å], GLN63[2.46 Å], TRP104[3.36 Å, 4.03 Å], VAL105[3.90 Å, 3.99 Å]	8
Indomethacin		-7.3	GLN1[2.67 Å], PRO46[2.96 Å], GLU47[3.40 Å, 4.00 Å], PHE106[3.27 Å], GLY107[2.21 Å]	6
Naproxen		-6.8	ARG25[15.76 Å], HSD100[3.29 Å], SER120[2.70 Å], SER121[2.27 Å], ALA122[2.25 Å]	5
Ibuprofen		-6.8	GLN1[2.39 Å], ARG25[15.81 Å], SER121[2.16 Å], ALA122[2.14 Å]	4
Aspirin		-5.9	ARG34[4.83 Å, 2.97 Å], TRP99[3.06 Å]	3

Table 3. Anti-inflammatory activity of test compounds

Treatment	Mean paw volume (ml)			
	0 hr	1 hr	2 hr	4hr
Inflammatory control (receives 0.5% CMC)	0.35 ± 0.04	0.56 ± 0.05	0.63 ± 0.03	0.70 ± 0.04
Diclofenac (15mg/kg) p. o.	0.33 ± 0.01	0.48 ± 0.02	0.50 ± 0.04**	0.33 ± 0.03***
Celecoxib (6 mg/kg) p.o.	0.38 ± 0.03	0.55 ± 0.01	050 ± 0.04**	0.40 ± 0.04***
5a (50mg/kg) p. o.	**0.35 ± 0.02**	**0.55 ± 0.05**	**0.58 ± 0.03**	**0.48 ± 0.03***
5b	0.21 ± 0.03	0.40 ± 0.03	0.36 ± 0.03*	0.29 ± 0.03***
5c	**0.35 ± 0.05**	**0.48 ± 0.04**	**0.53 ± 0.03***	**0.50 ± 0.05***
5d	0.24 ± 0.03	0.42 ± 0.03	0.31 ± 0.01*	0.23 ± 0.02***
5e	0.27 ± 0.01	0.44 ± 0.02	0.33 ± 0.04*	0.29 ± 0.01***
5f	0.23 ± 0.04	0.42 ± 0.02	0.34 ± 0.02*	0.27 ± 0.03***
5g	0.26 ± 0.01	0.47 ± 0.03	0.32 ± 0.04*	0.25 ± 0.03***
5h	0.25 ± 0.04	0.41 ± 0.01	0.32 ± 0.04*	0.24 ± 0.01***
5i	0.22 ± 0.02	0.41 ± 0.04	0.34 ± 0.01*	0.22 ± 0.02***
5j	0.24 ± 0.03	0.43 ± 0.05	0.36 ± 0.04*	0.21 ± 0.02***
5k	0.24 ± 0.01	0.45 ± 0.07	0.31 ± 0.03*	0.25 ± 0.04***
5l	0.26 ± 0.03	0.44 ± 0.03	0.33 ± 0.01*	0.29 ± 0.05***

Values are expressed as mean ±SEM of six rats in each group. Statistically significant ***p<0.001, **p<0.01,*p<0.05 compared to inflammation control.

Table 4. Inflammation Percentage inhibition of test compounds

Treatment	Percent inhibition		
	1 hr	2 hr	4hr
Diclofenac(15mg/kg) p. o.	14.29	20.63	52.85
Celecoxib (6mg/kg) p.o.	1.79	20.63	42.86
5a (50mg/kg) p. o.	**14.29**	**17.87**	**48.57**
5b	2.49	7.94	21.43
5c	**5.36**	**20.63**	**42.86**
5d	4.12	7.92	16.41
5e	7.16	8.92	21.44
5f	5.36	7.46	28.51
5g	2.71	7.94	21.42
5h	5.12	7.71	31.41
5i	4.13	17.12	28.52
5j	4.36	17.46	28.57
5k	6.79	5.92	21.45
5l	4.72	9.94	31.43

Table 5: The docking HOMO and LUMO value of **5a**, **5c** test compounds, and standard **Celecoxib**

Code	HOMO Energy	LUMO Energy	Energy Gap
5a	0.28634	0.21216	2.018541652
5c	0.30413	0.23108	1.98776355
Celecoxib	0.30864	0.17735	3.57253219

Table 6: The ADME and physicochemical properties of **5a**, **5c** test compounds, and standard **Celecoxib**

Code	Violation of Lipinski's rule	The polar surface area (TPSA)	Gastro intestinal (GI) absorption	bioavailability score	Synthetic accessibility
5a	Yes	77.81 Å²	High	+0.55	4.99
5c	Yes	123.63 Å²	High	+0.17	5.11
Celecoxib	No	86.36 Å²	High	+0.55	2.74

Figures
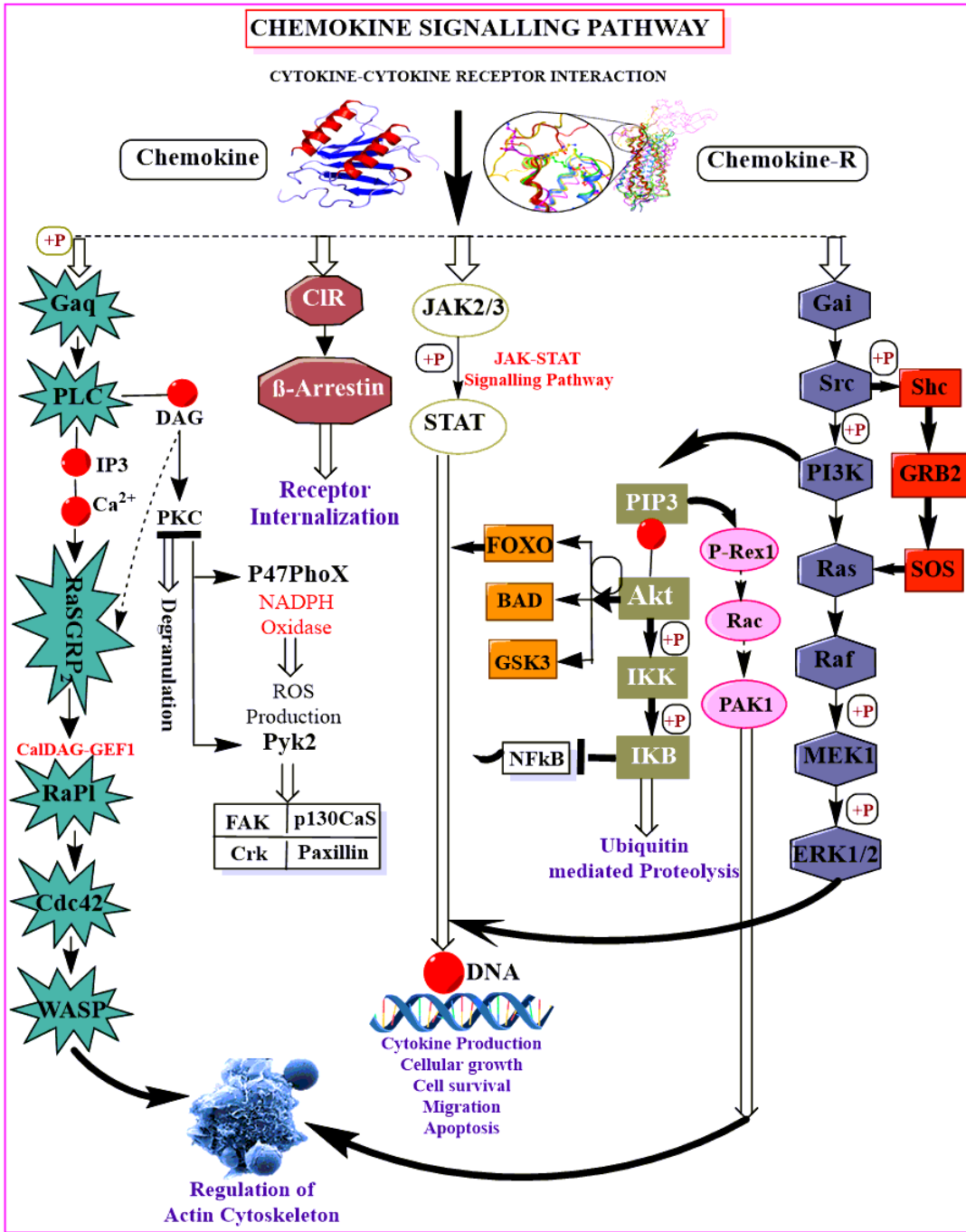
Figure 1

The CXCR6/Chemokine signalling pathway
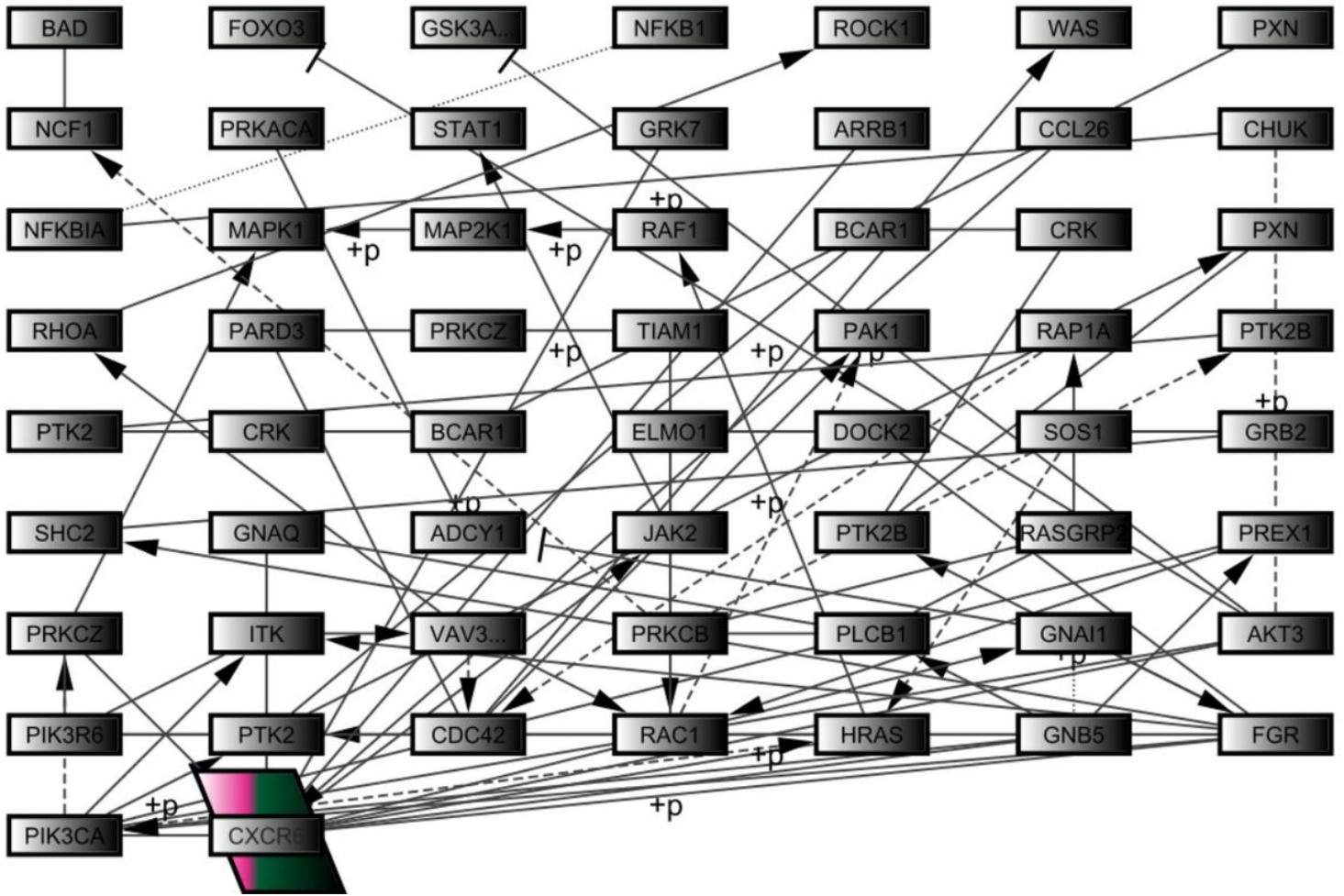
Figure 2

The CXCR6/Chemokine pathway with nodes and edges interaction
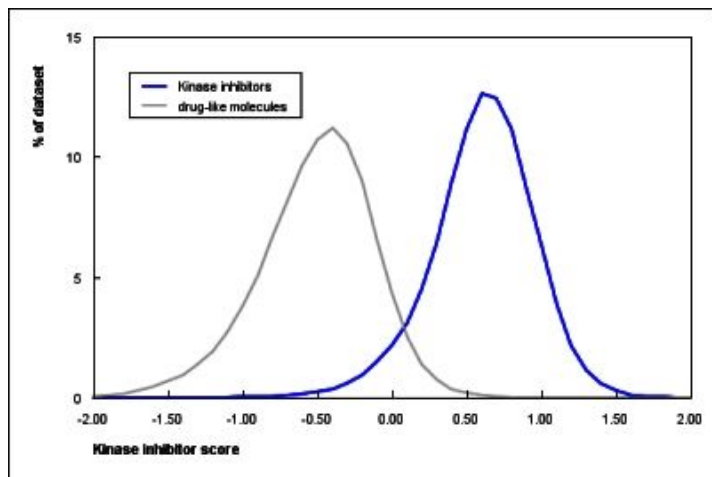
Figure 3

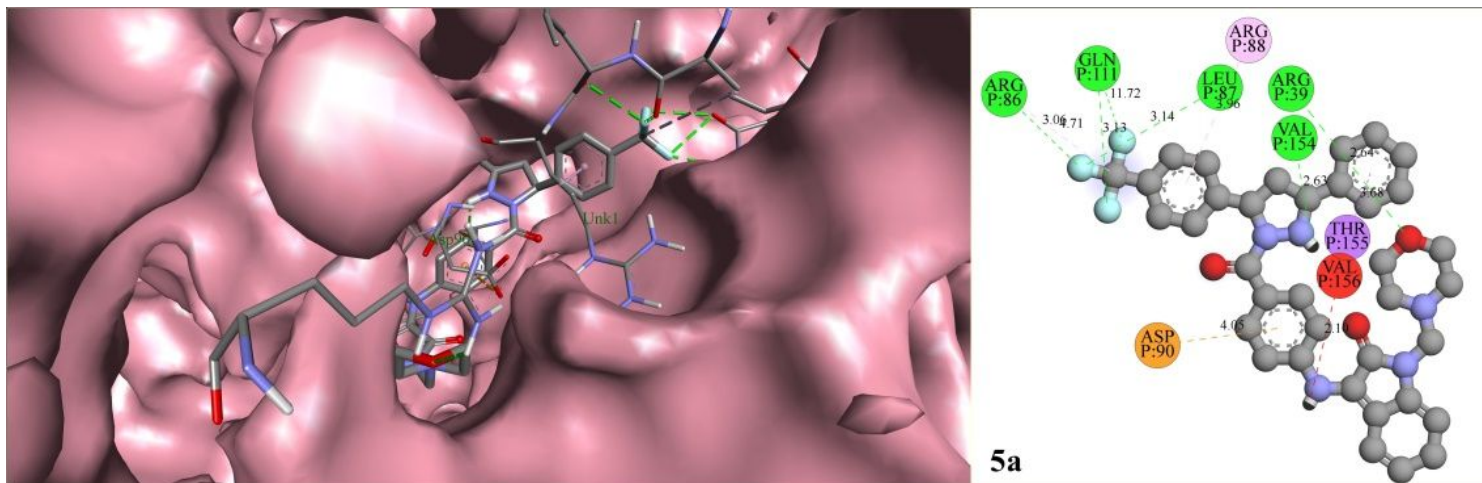The druglikeness graph of **5a-5l**

Figure 4

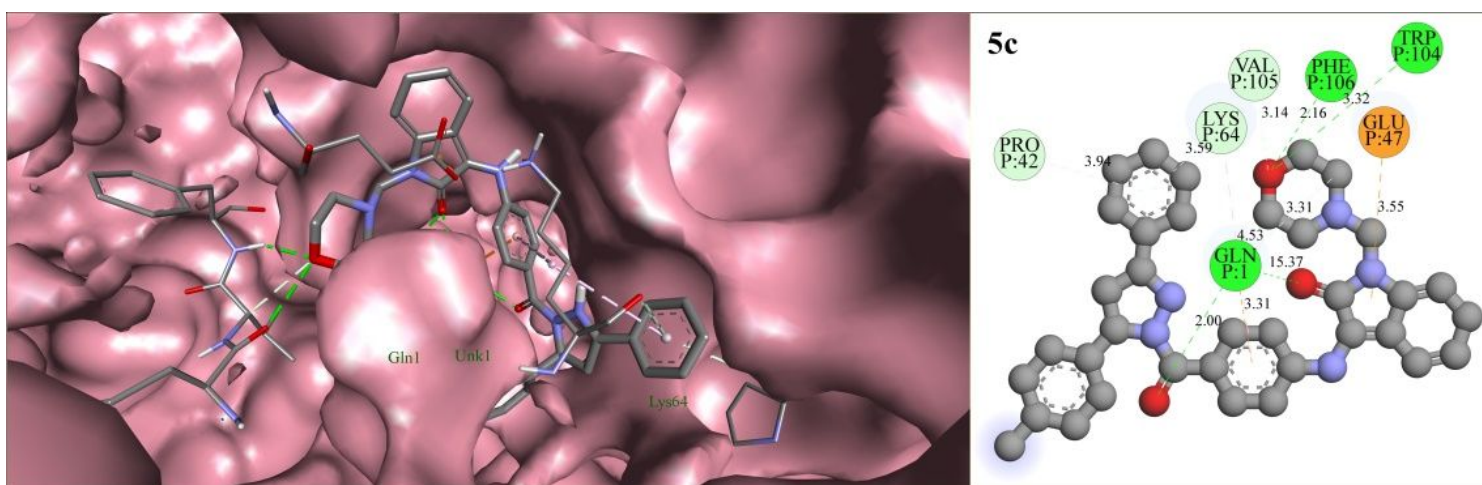The binding interactions, 2D and 3D model of test compound **5a**

Figure 5

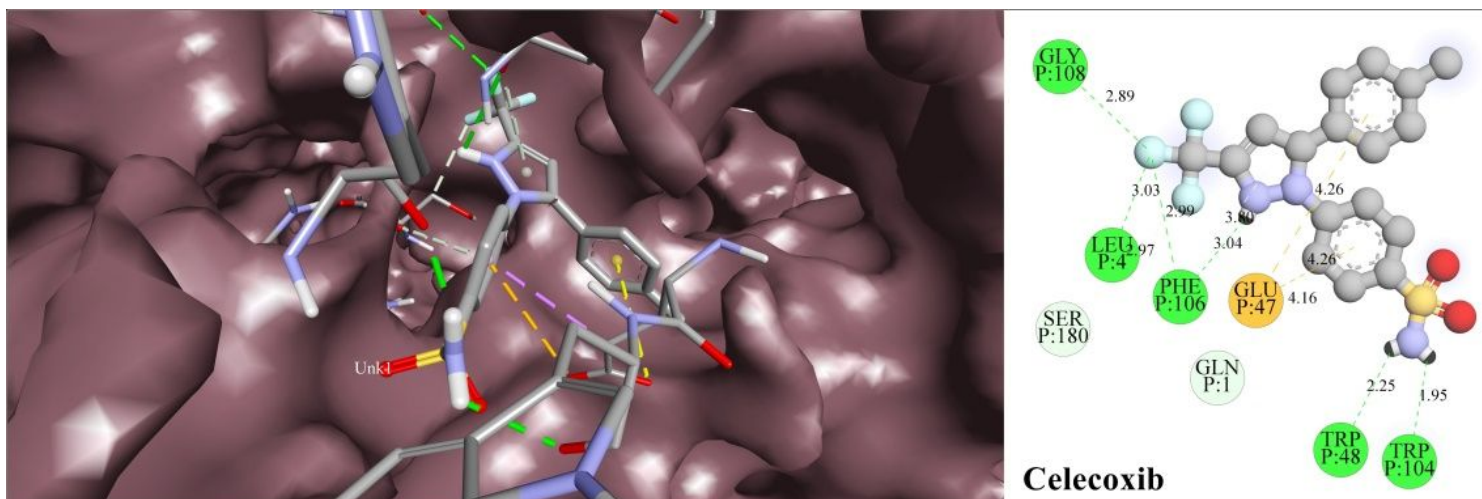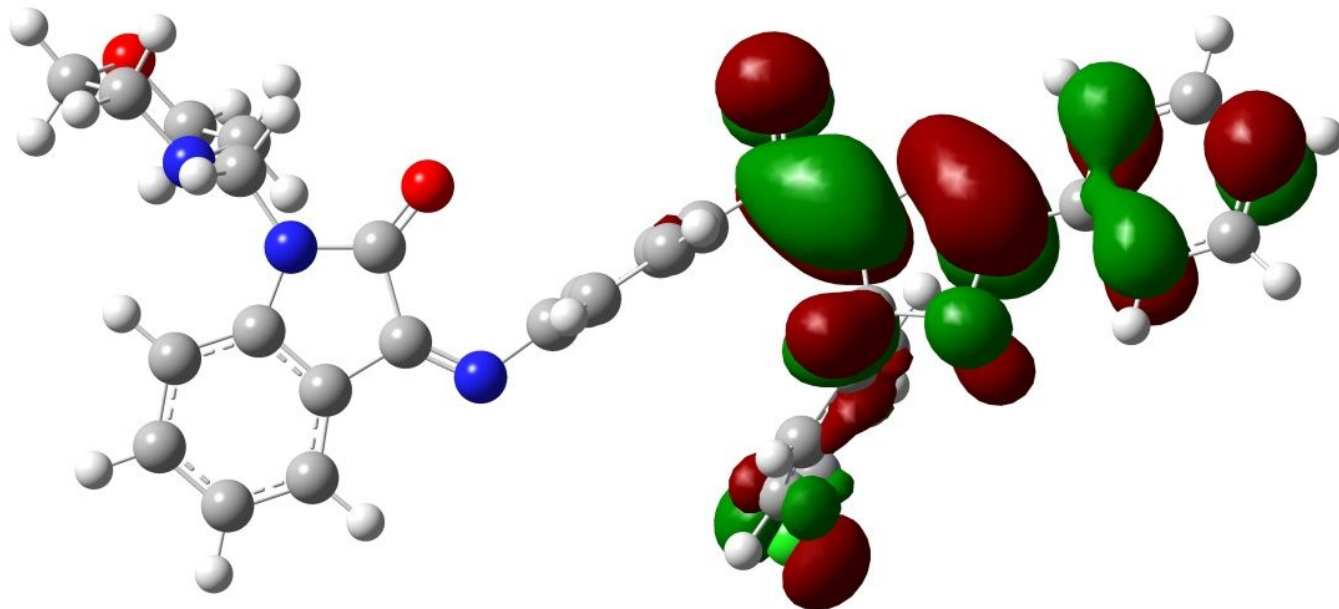The binding interactions, 2D and 3D model of test compound **5c**

Figure 6

The binding interactions, 2D and 3D model of test compound **Celecoxib**

Figure 7

The anti-inflammatory activity of 3-(4-(5-(4-Chlorophenyl)-3-phenyl-4,5-dihydro-1*H*-pyrazole-1-carbonyl)phenylimino)-1-(morpholinomethyl)indolin-2-one (**5a**)

5a HOMO

5a LUMO
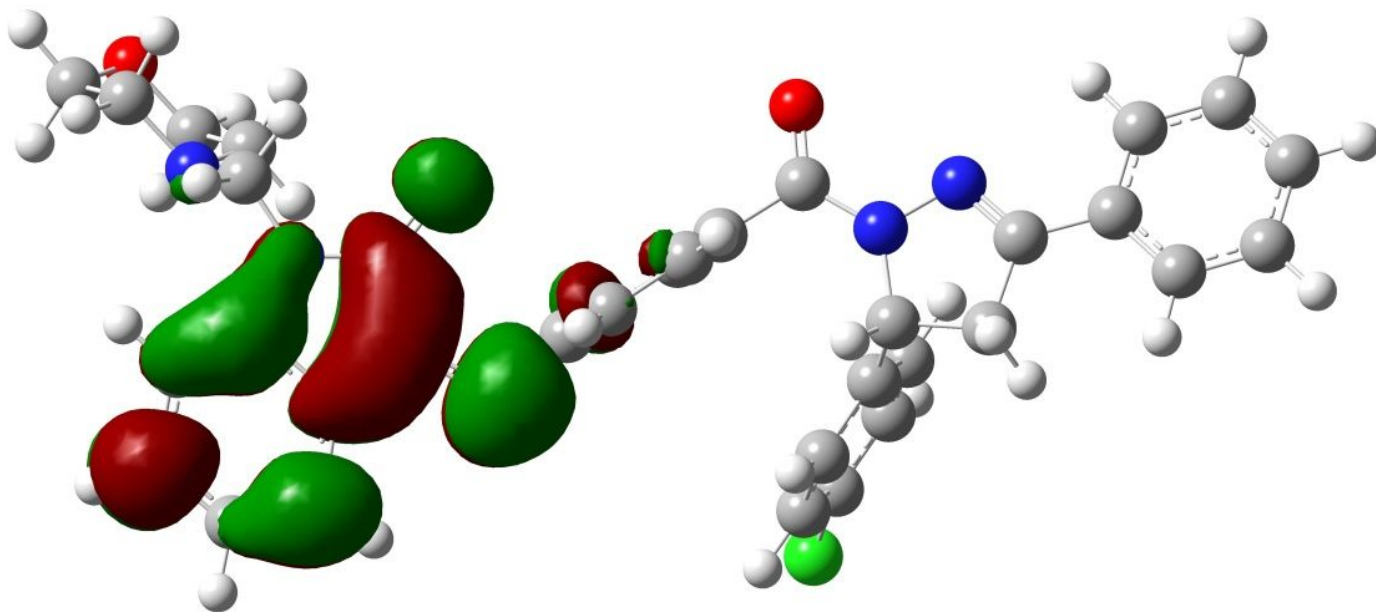
Figure 8

The energy values of HOMO and LUMO of test compound **5a**

5c HOMO

5c LUMO
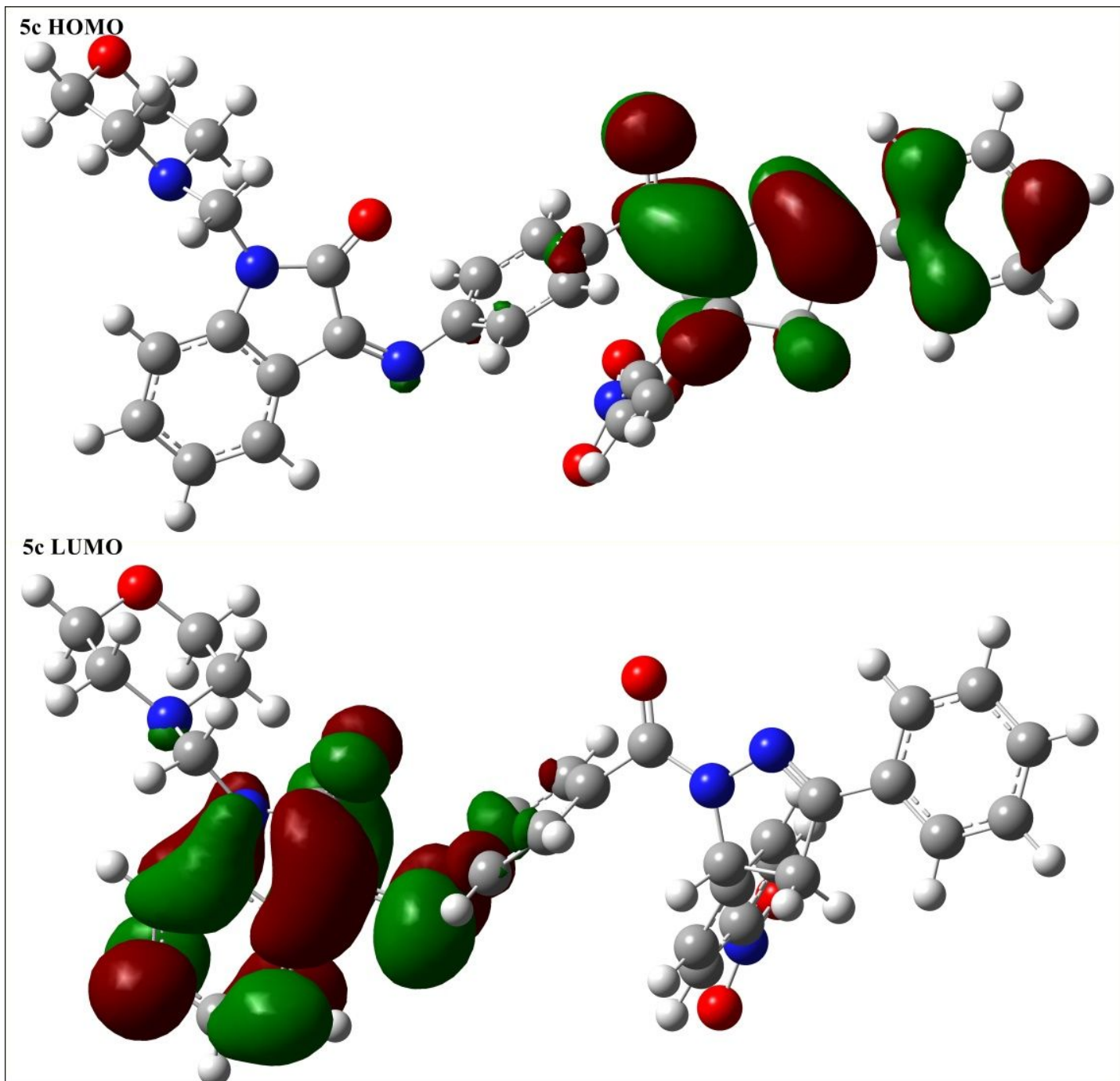
Figure 9

The energy values of HOMO and LUMO of test compound **5c**

Celecoxib HOMO
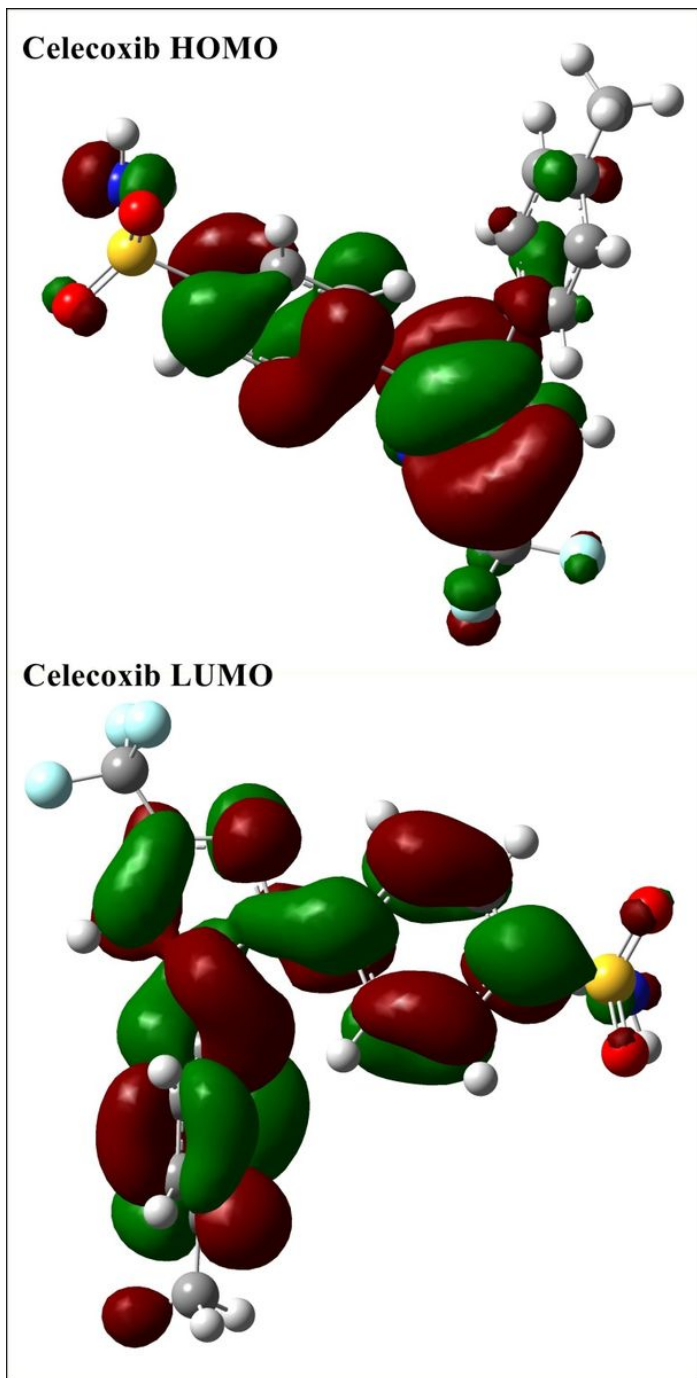
Celecoxib LUMO

Figure 10

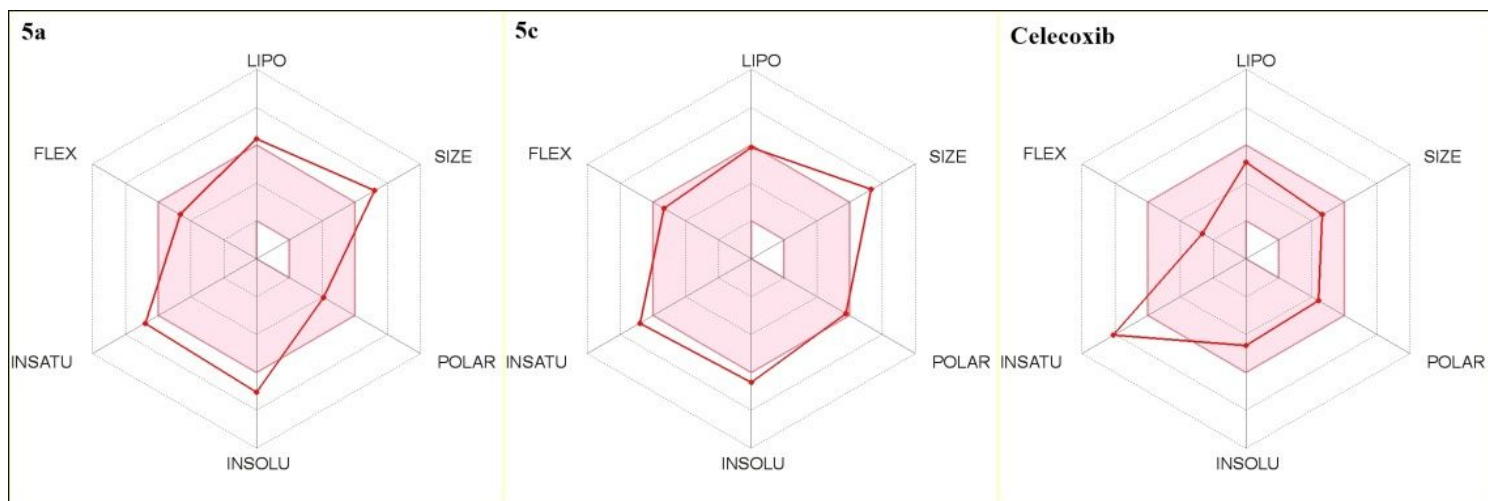The energy values of HOMO and LUMO of test compound **Celecoxib**

Figure 11

The Lipinski properties of **5a**, **5c** and standard **Celecoxib**
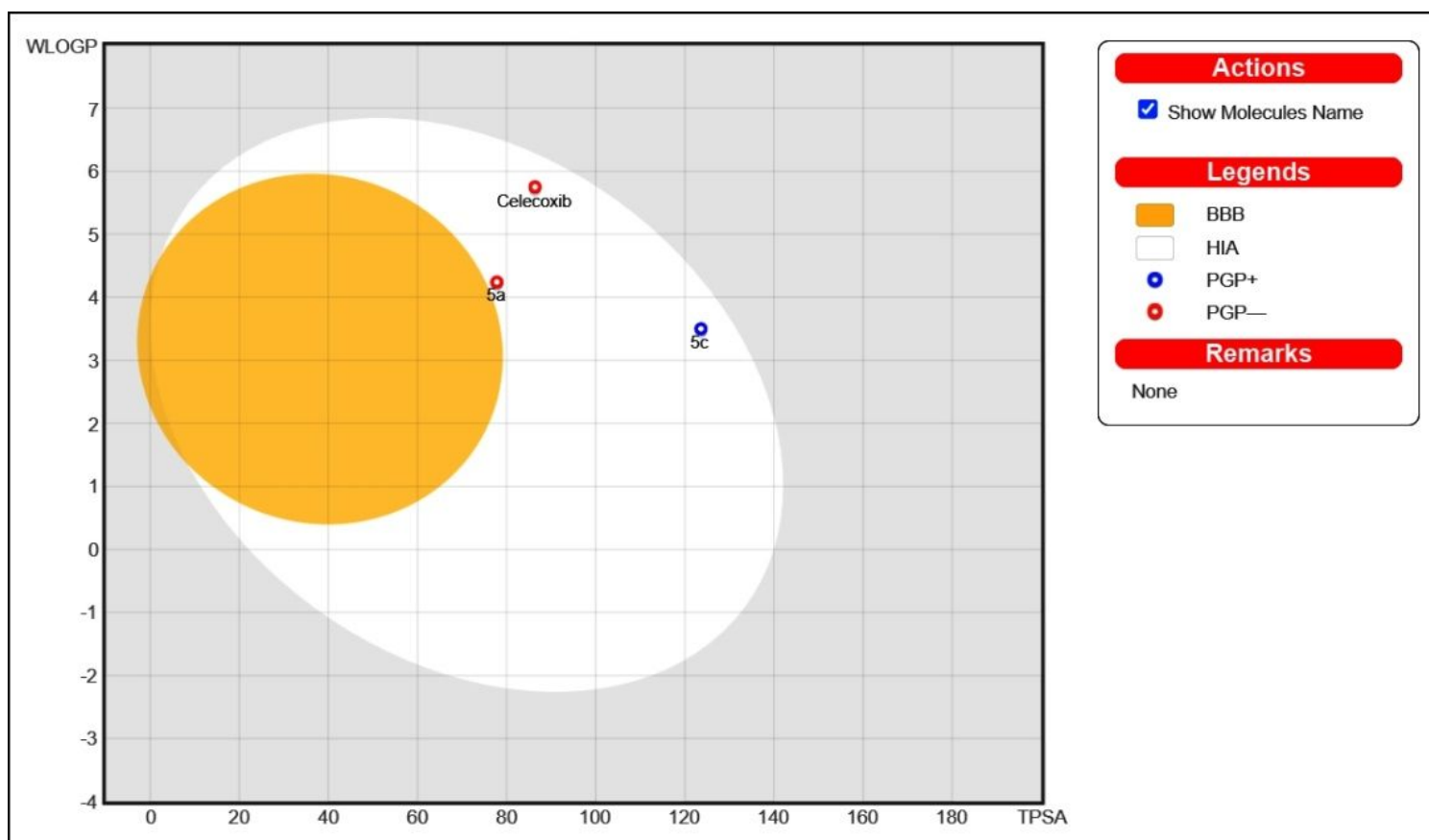

Figure 12

The egg-boiled model of **5a**, **5c** and standard **Celecoxib**